Copy No. _____

Defence Research and Development Canada
Recherche et développement pour la défense Canada

DEFENCE R&D DÉFENSE

Wideband detection and classification of practice limpet mines against various backgrounds

John A. Fawcett
Richard Fleming

Defence R&D Canada – Atlantic

Technical Memorandum
DRDC Atlantic TM 2008-079
July 2008

Canada

This page intentionally left blank.

Wideband detection and classification of practice limpet mines against various backgrounds

John Fawcett
Richard Fleming

Defence R&D Canada – Atlantic

Technical Memorandum
DRDC Atlantic TM 2008-079
July 2008

Principal Author

Original signed by John Fawcett

John Fawcett

Approved by

Original signed by David Hopkin

David Hopkin

Head/ Maritime Asset Protection

Approved for release by

Original signed by James L. Kennedy

James L. Kennedy

A/Chair Document Review Panel

Abstract

In this experiment we placed actual practice limpet mines on a one-metre diameter disc which was suspended in the DRDC Atlantic acoustic calibration tank from a rotator pole. Two different discs were considered: one, aluminum and the other fibreglass. These discs were then rotated under a fixed multi-mode pipe projector (MMPP) and hydrophone. The geometry was arranged so that the mineshapes would appear directly under the projector/hydrophone during the rotation. The measurements were made at 2 different disc-projector offsets and for a slightly bistatic arrangement. Various different incident pulses were considered corresponding to different frequency bands. It is shown that the mineshapes are often easily discriminated from the surrounding disc response, in terms of both the echo travel time and the characteristics (temporal and spectral) of the echoes.

Résumé

Au cours de l'expérience, nous avons placé des mines ventouses réelles d'entraînement sur un disque d'un diamètre de 1 m suspendu dans le réservoir acoustique d'étalonnage de RDDC Atlantique à l'aide d'une perche rotative. Deux disques ont été examinés : un en aluminium et l'autre, en fibre de verre. Les disques ont été tournés au-dessous d'un projecteur à tube multimode fixe (MMPP) et d'un hydrophone. La géométrie a été configurée de sorte que les formes des mines paraissent directement sous le projecteur/l'hydrophone durant la rotation. Des mesures ont été prises à deux décalages du projecteur à disques et pour un arrangement légèrement bistatique. Différentes impulsions incidentes correspondant à différentes bandes de fréquences ont été étudiées. On montre que les formes des mines sont souvent faciles à distinguer de la réponse ambiante des disques en termes du temps de parcours et des caractéristiques (temporelles et spectrales) des échos.

This page intentionally left blank.

Executive summary

Wideband detection and classification of practice limpet mines against various backgrounds:

J. Fawcett; R. Fleming; DRDC Atlantic TM 2008-079; Defence R&D Canada – Atlantic; July 2008.

Introduction or background: The sonar detection of small mines (or other objects) placed upon a reflective surface such as a ship's hull or a piling is a challenging problem. It may be possible to detect the object with a bathymetric sonar on the basis of the relative altitude of the object with respect to the background. However, various protuberances, ribs, etc could also cause altitude variations. High-frequency imaging sonars can provide a map of the high-frequency reflectivity of the surface and any attached objects. The approach of this report is to look for distinctive or anomalous wideband spectral signatures as a means of distinguishing mine regions from the background. The wide bandwidth yields valuable detection and classification information. In addition, the lower frequencies can penetrate into objects and there may be scattering from internal structures. In a previous report, the feasibility of this method was illustrated with some simple improvised shapes placed upon a sheet of fibreglass. In the present report, we consider some actual practice limpet mines placed upon 2 different background discs, which are rotated in a controlled fashion below a fixed projector and hydrophone. As well, 3 identically shaped objects with different interior fills are considered.

Results: It is shown that the mineshapes can be successfully classified with respect to a background reflector using the temporal or spectral information of the echo from a single sonar ping. This was even true in the case that the objects had identical shape but only different interior materials. This can be done independently of the background signature. Instead of direct classification, the mineshapes can also be easily identified on the basis of "change" with respect to the neighbouring signatures of the disc/plate region.

Significance: This experiment indicates the potential of using wideband scattering information, perhaps in conjunction with imaging sonar, as an acoustic tool for identifying mines upon a ship hull, on a pier, or other submerged surfaces.

Future plans: We would like to perform trials with the projector/hydrophone system on a remotely operated vehicle with mine-like objects deployed on the surface of a ship or pier. We would also like to use mineshapes with inert fills that closely mimic the material properties of explosives.

Sommaire

Wideband detection and classification of practice limpet mines against various backgrounds:

J. Fawcett; R. Fleming; DRDC Atlantic TM 2008-079; R & D pour la défense Canada – Atlantique; Juillet 2008.

Introduction: La détection par sonar de petites mines ou d'autres objets placés sur une surface réfléchissante, comme la coque d'un navire ou un pilotis, constitue un problème difficile. Avec un sonar bathymétrique, il peut être possible de détecter un objet à partir de sa « hauteur » par rapport à son fond. Toutefois, diverses protubérances, membrures et autres structures peuvent causer des variations de la hauteur. Les sonars imageurs haute fréquence permettent de dresser une carte de la réflectivité haute fréquence de la surface et de tout objet attaché. Dans le présent rapport, nous étudions l'utilisation des signatures spectrales à large bande distinctes ou anormales pour distinguer les régions des mines du fond sur lequel elles sont placées. La grande largeur de bande donne des données précieuses pour la détection et la classification. En outre, les fréquences inférieures peuvent pénétrer dans les objets, et il peut y avoir diffusion à partir des structures internes. Dans un rapport antérieur, la faisabilité de cette méthode a été illustrée à l'aide de certaines formes improvisées simples placées sur une feuille de fibre de verre. Dans le présent rapport, nous examinons certaines mines ventouses réelles d'entraînement placées sur deux disques de référence, que l'on tourne de façon contrôlée au-dessous d'un projecteur fixe et d'un hydrophone. En outre, trois objets de forme identique, remplis de matières différentes, sont examinés.

Résultats: On montre que les formes des mines peuvent être classées avec succès par rapport à un réflecteur d'arrière-plan à l'aide des données temporelles ou spectrales des échos d'une seule impulsion de sonar. Cette classification est possible même dans le cas où les objets ont une forme identique, et que la seule différence est leur matériau de remplissage. Elle peut se faire indépendamment de la signature de fond. Au lieu d'une classification directe, il est aussi possible d'effectuer une identification des formes de mines en fonction de la « variation » par rapport aux signatures voisines de la région des disques/plaques.

Importance: L'expérience montre les possibilités qu'offre l'utilisation des données de diffusion en bande large – possiblement de concert avec un sonar imageur – comme outil acoustique d'identification des mines sur la coque d'un navire, une jetée ou d'autres surfaces submergées.

Perspectives: Nous voulons mener des essais à l'aide du système de projecteur/ d'hydrophone sur un véhicule télécommandé et d'objets analogues à des mines posées sur la surface d'un navire ou d'une jetée. Nous voulons aussi nous servir de formes de mines remplies de matières inertes qui reproduisent assez bien les propriétés matérielles d'explosifs.

Table of contents

List of figures

Acknowledgements

The authors would like to thank Mark Rowsome for his preparation of the aluminum and fibreglass discs. They are also grateful to PO1 Keith Musselman of Fleet Diving Unit Atlantic for his help in obtaining the loan of the practice limpet mines.

This page intentionally left blank.

1 Introduction

The detection of mines or explosive devices planted on a ship's hull or on a piling is currently a research topic of much interest. High frequency sonars may provide an image of the area of interest or a bathymetric sonar may be able to resolve the height difference caused by an object placed on a surface. However, on the basis of high-frequency reflectivity or altitude measurements alone, it is anticipated that there is potential for many false alarms. The approach of this report is to investigate whether it is possible to reliably distinguish echoes of interest from background echoes utilizing a wideband incident pulse.

In order to generate a wideband sonar signal we will use a small high frequency multi-mode pipe projector (HF MMPP) which is capable of yielding a very wideband pulse with significant power. The projector that is used has been described in previous reports [1-3]. In [3] a simplified version of the experiments of this report was carried out. An improvised mine-like object (and variations of this object) was placed upon a sheet of fibreglass and a projector/hydrophone system was manually rotated over the sheet and object. It was shown in [3] that the objects' and the fibreglass sheet's signatures could be accurately classified.

The experiments of this report are similar in concept to those earlier experiments. However, in this case, 3 practice limpet mineshapes were borrowed from Fleet Diving Unit Atlantic (FDU-A) and were affixed to circular discs of either aluminum or fibreglass. Although realistic in shape, these practice limpet mineshapes are not indicative of the internal structure of real limpet mines. These 1-m diameter discs were then attached to a rotation assembly which allowed the disc to be mechanically rotated below the projector/hydrophone at a constant angular velocity. As well, some other targets were considered. In particular, we constructed 3 identically-shaped, small mine-like objects differing only in their interior fill. This process was done for both types of discs, at 2 projector offsets, and for various types of incident pulses. Other rotations were done in a bistatic projector/hydrophone mode. In total, 34 rotations were carried out.

Representative data from the various rotations will be presented in both the temporal and spectral domains. The echoes from the various targets and the plates will be considered. The automated detection of echoes of interest will be investigated and it will be shown that individual echoes can be successfully classified.

2 Experimental Setups and Targets

2.1 Set-up

DRDC Atlantic's acoustic calibration tank (ACT) was equipped with suspended 5.91 mm thick discs (1 m diameter) of fibreglass and aluminum in order to provide a simulated submerged boat hull upon which a simulated "mine" and a series of other reflectors could be attached. One of these discs was attached to one of the ACT rotating stations to permit controlled rotation of the disc under the hydrophone- projector assembly thereby simulating transit of the projector-hydrophone over a fixed surface. In total, 34 measurements were taken as the 1 m disc was rotated through 360° with targets mounted on the disc being ensonified. Three distinct variations of the experimental set-up were employed. Figure 1 shows the vertical alignment of the HF MMPP and B&K 8104 hydrophone (measurements 1 to 14 and 17 to 22). Figure 2 shows the bistatic offset arrangement of the B&K 8104 hydrophone with respect to the HF MMPP (measurements 15 and 16). Figure 3 shows the vertical alignment of the HF MMPP and a B&K 8103 hydrophone (measurements 23 to 34). Various spacings of the HF MMPP/hydrophone pairings from the target mounting plate were used ranging from 40 to 60 cm.

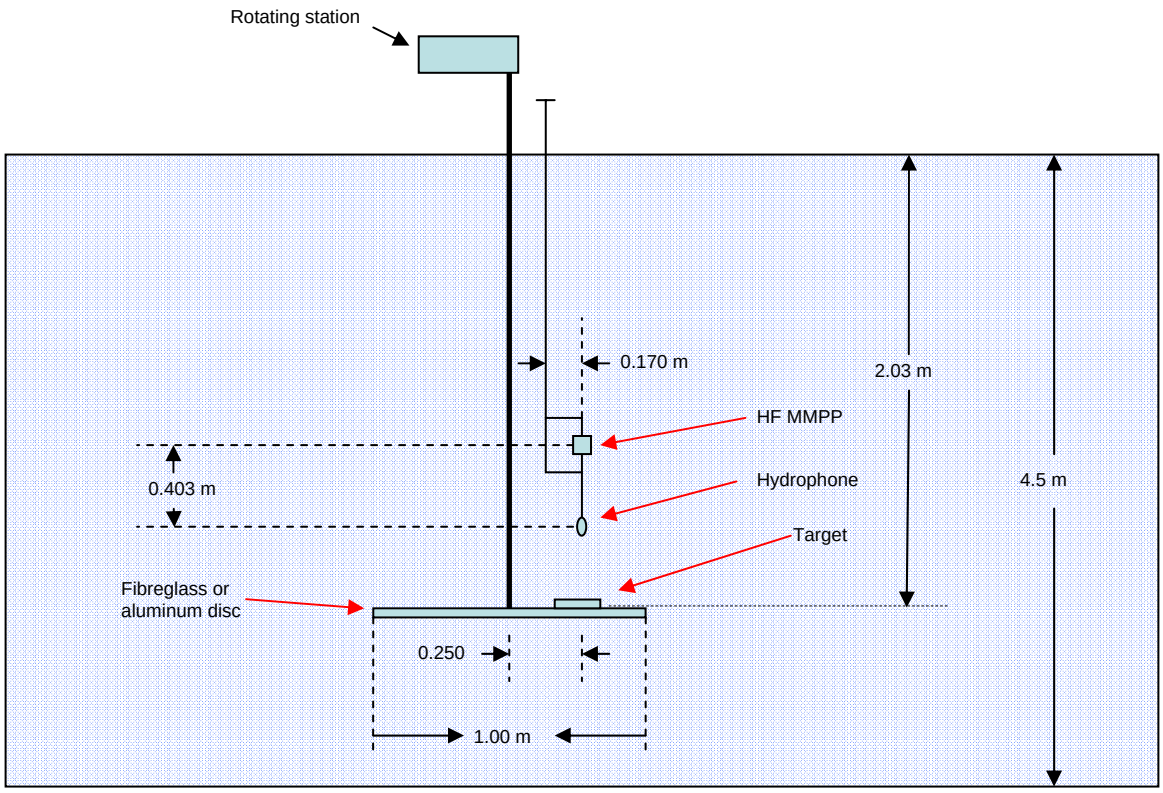

Figure 1 Drawing of ACT test set-up for HFMMPP/B&K 8104 hydrophone in-line topology.

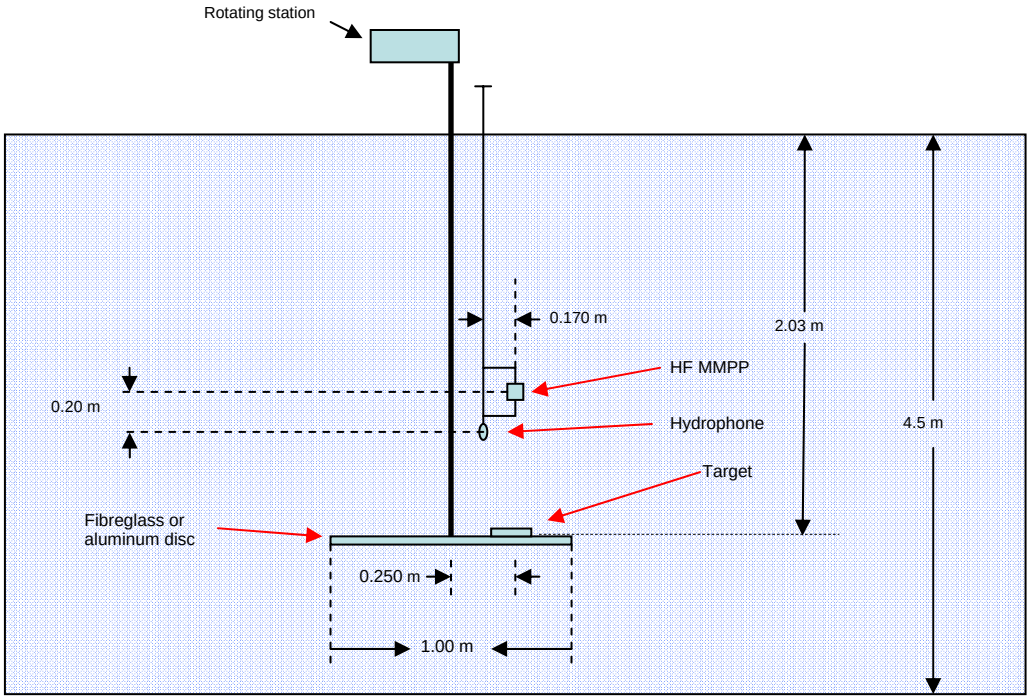

Figure 2 Drawing of ACT set-up with bistatic arrangement of B&K 8104 hydrophone with respect to the HF MMPP.

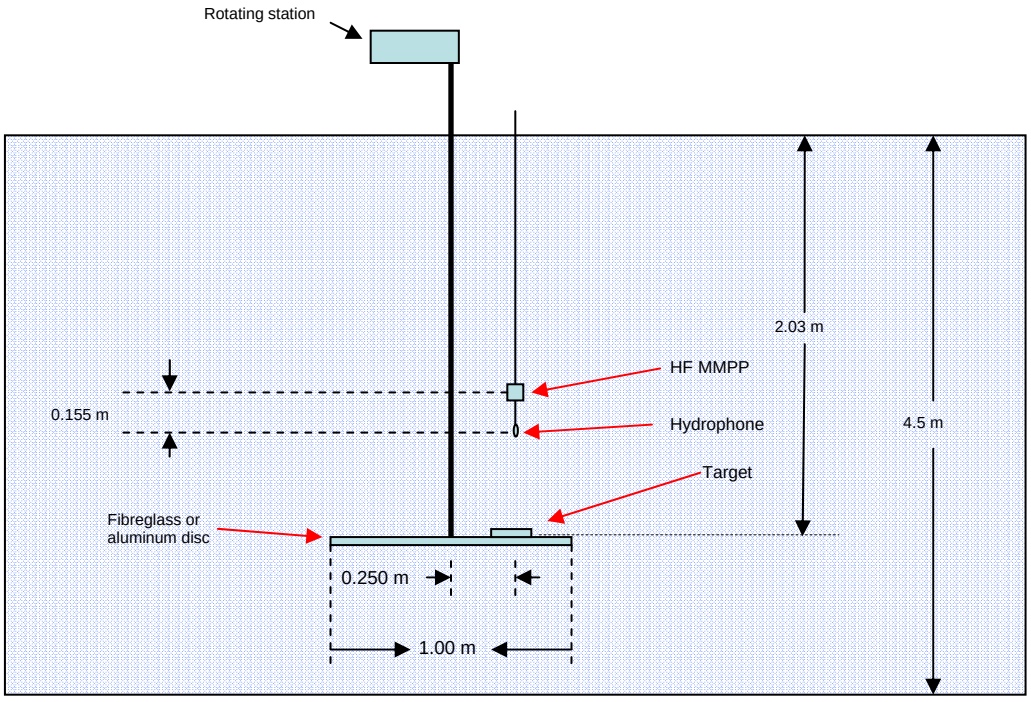

Figure 3 Drawing of ACT set-up with vertical arrangement of B&K 8103 hydrophone with respect to the HF MMPP.

A high frequency multi-mode pipe projector was employed in its endfire configuration to provide wideband acoustic energy (see Figure 4). HF MMPP serial number 1 was used for measurements 1 to 5 but was replaced with the slightly better performing unit number 3 for the remainder of the measurements.

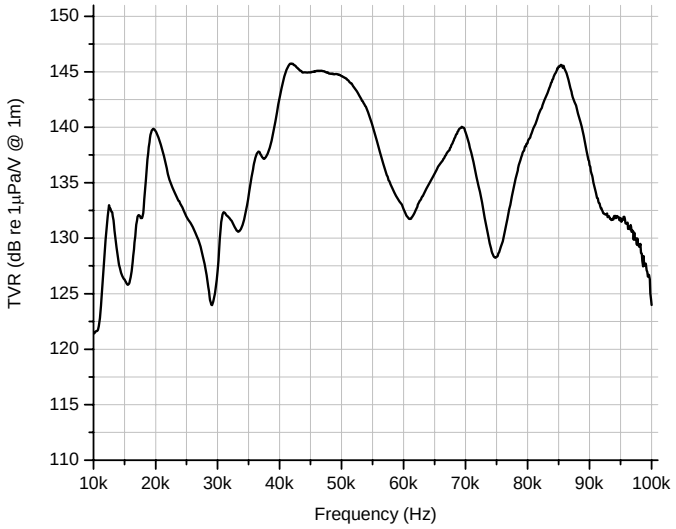

Figure 4 HF MMPP endfire transmitting voltage response.

A B&K™ 8104 hydrophone (serial number 861) was mounted by a fibreglass rod near the HF MMPP in the first two set-ups. This hydrophone provided good receive sensitivity over the band of interest (see Figure 5). The first of the hydrophone/HF MMPP arrangements can be seen in figure 6. A B&K 8103 (serial number 387) was used in the final vertical arrangement as it has a small acoustic cross-section and better high frequency response. This arrangement can be seen in Figure 7.

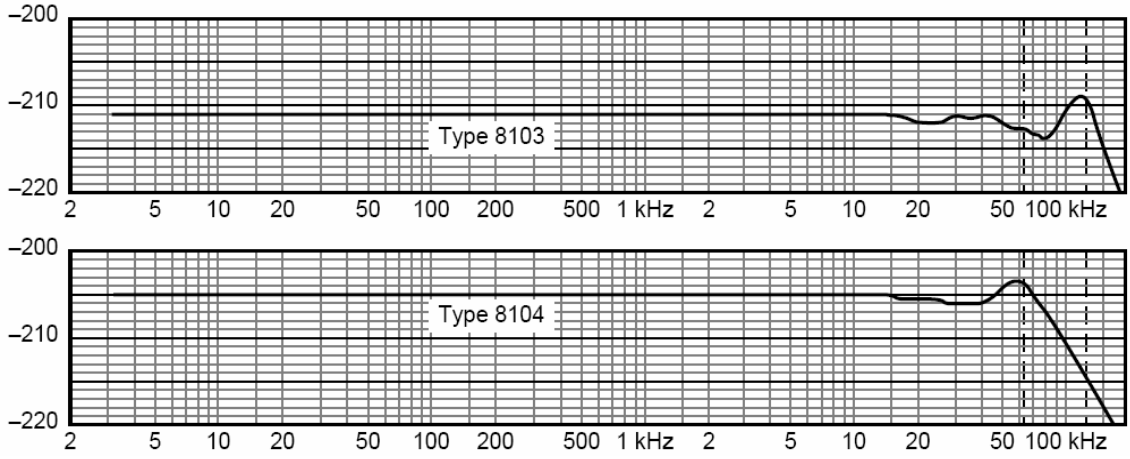

Figure 5 Typical receive sensitivity of B&K™ 8103 and 8104 hydrophones.

Sinc pulses were generated using a LabView™ virtual instrument called the Pulse Echo Recorder which was developed at DRDC Atlantic [1]. The sinc pulses were amplified by an Instruments Incorporated Model L-2 amplifier. Drive voltage was on the order of 47 Vrms resulting in a post-spectral correction source level of 112 dB re 1µPa @ 1m/√Hz.

Figure 6 Detail of HF MMPP/ hydrophone for first experimental set-up.

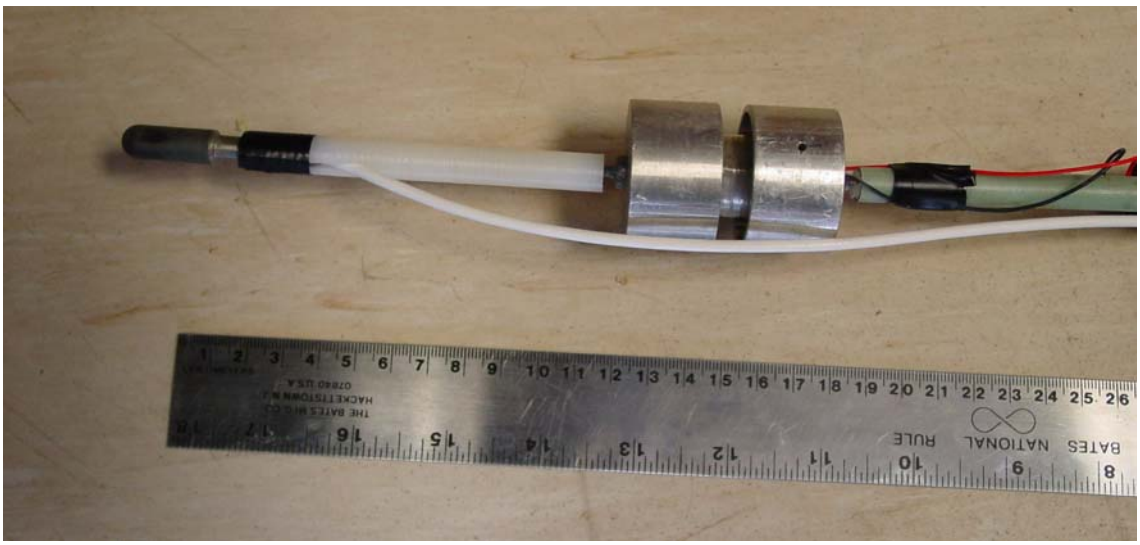

Figure 7 Detail of HF MMPP/ hydrophone for third experimental set-up.

2.2 Targets

Various targets, including naval practice limpet mines, and combinations of targets were employed in the measurements taken. We now describe these objects in some detail.

2.2.1 Practice limpet mines

The three naval practice limpet mines borrowed from FDU-A were an aluminum right-cylindrical segment unit, a polymer-bodied unit and an aluminum hemispherical unit (see Figures 8 and 9). Since internal composition of these units could not be ascertained, only outer dimensions and mine hull materials are described. Figures 10, 11, and 12 show the top view and dimensions of each of these practice limpet mines. Each mine is equipped with permanent magnets for attachment. The apex height of the practice limpet mine from the disc mounting surface is 7.8 cm for the polymer-bodied mine, 3.8 cm for the right-cylindrical mine and 14.6 cm for the hemispherical mine.

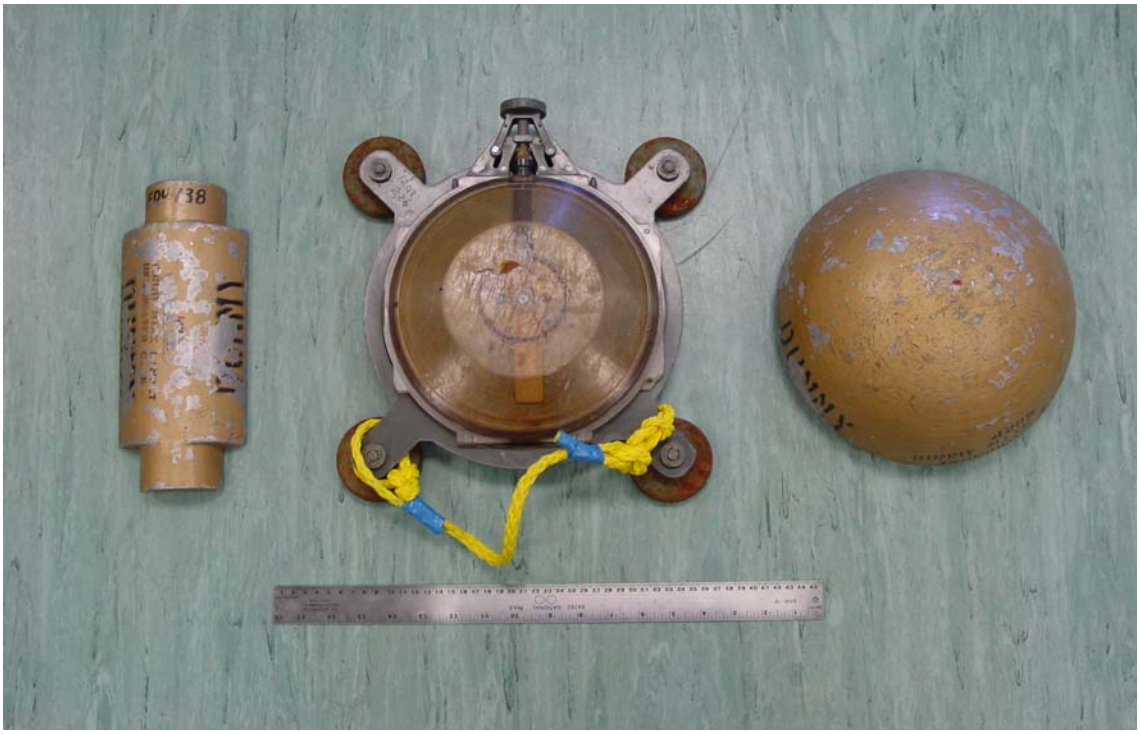

Figure 8 Top view of 3 practice limpet mines. L-R right cylindrical unit, polymer-bodied unit and hemispherical unit.

Figure 9 Side view of 3 practice limpet mines. L-R right cylindrical unit, polymer-bodied unit and hemispherical unit.

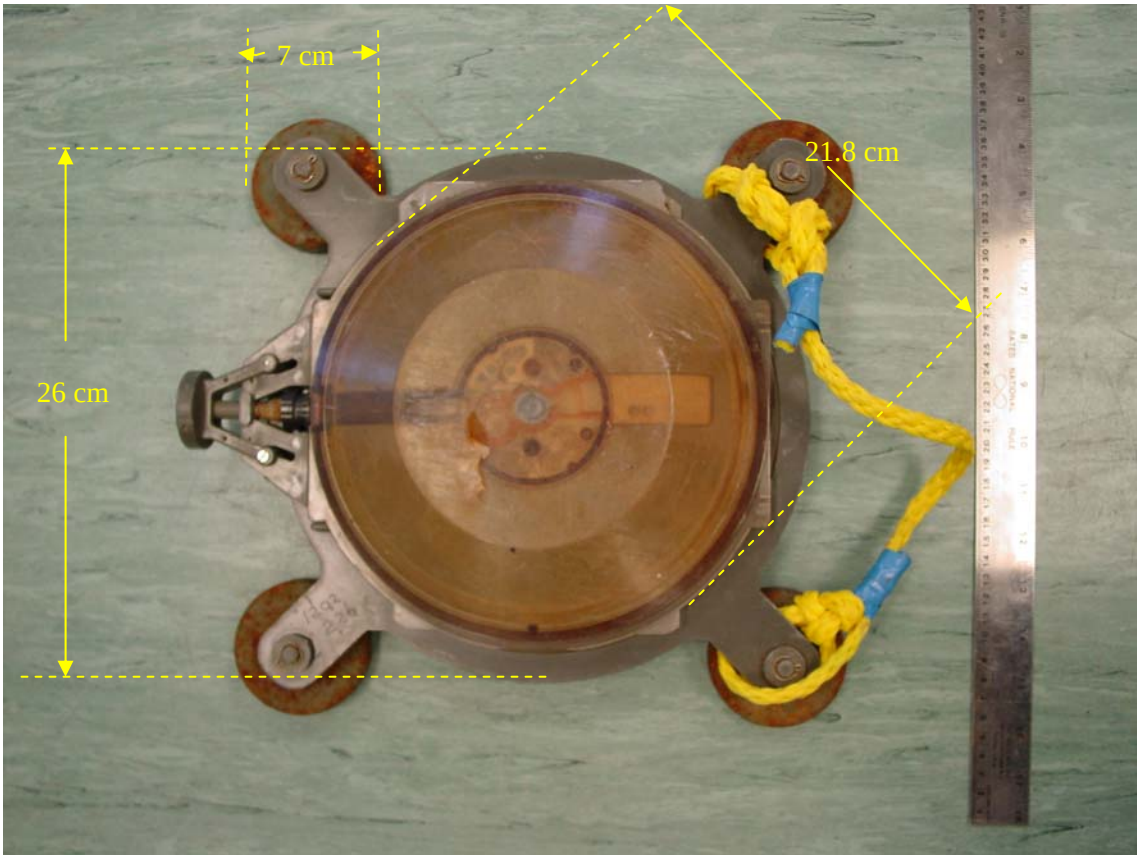

Figure 10 Polymer-bodied practice limpet mine top-view with dimensions.

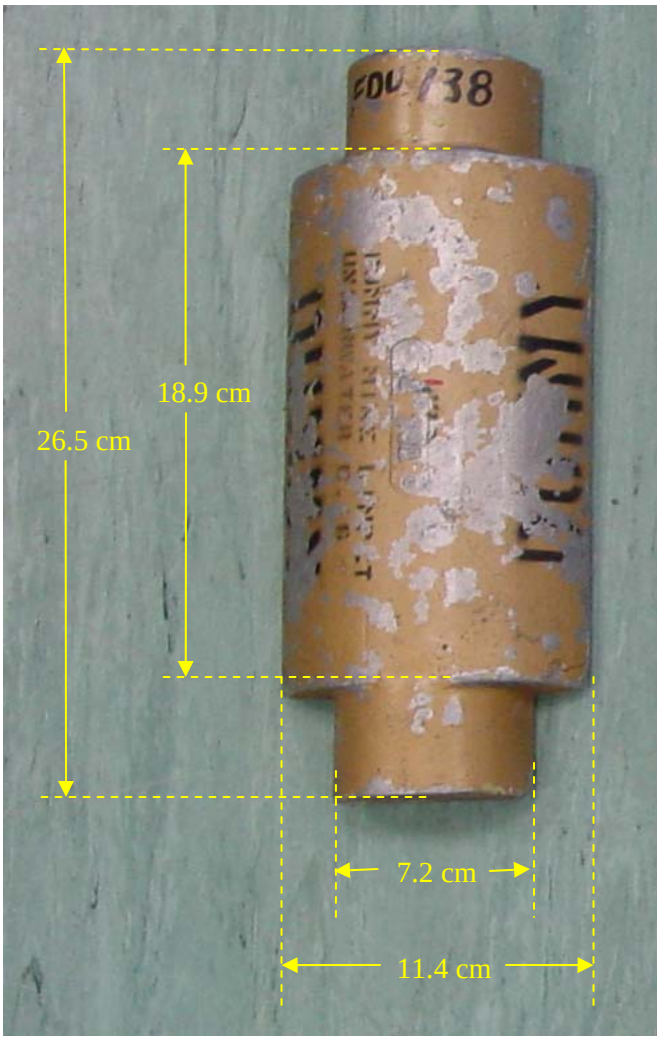

Figure 11 Right-cylindrical practice limpet mine top-view with dimensions.

Figure 12 Hemispherical practice limpet mine top-view with dimensions.

2.2.2 Rubber compound mineshapes

Three mineshapes were based on puck-shaped right cylinder composed of Loctite™ Rapid Rubber Repair compound (see Figure 13). All of these mineshapes were 10 cm in diameter and 2.5 cm in height. One mineshape was composed only of the rubber compound. Another mineshape contained a disc of aluminum that was 5.7 cm in diameter and 0.95 cm in height. This small aluminum disc was centered at the bottom of the mineshape and occupied approximately 12% of the shape's total volume. The third mineshape contained an even distribution of 400 g of 3.7 mm diameter steel ball bearings (see Figure 14). This third mineshape was also used in conjunction with the polymer-bodied practice limpet mine for some measurements (see Figure 15).

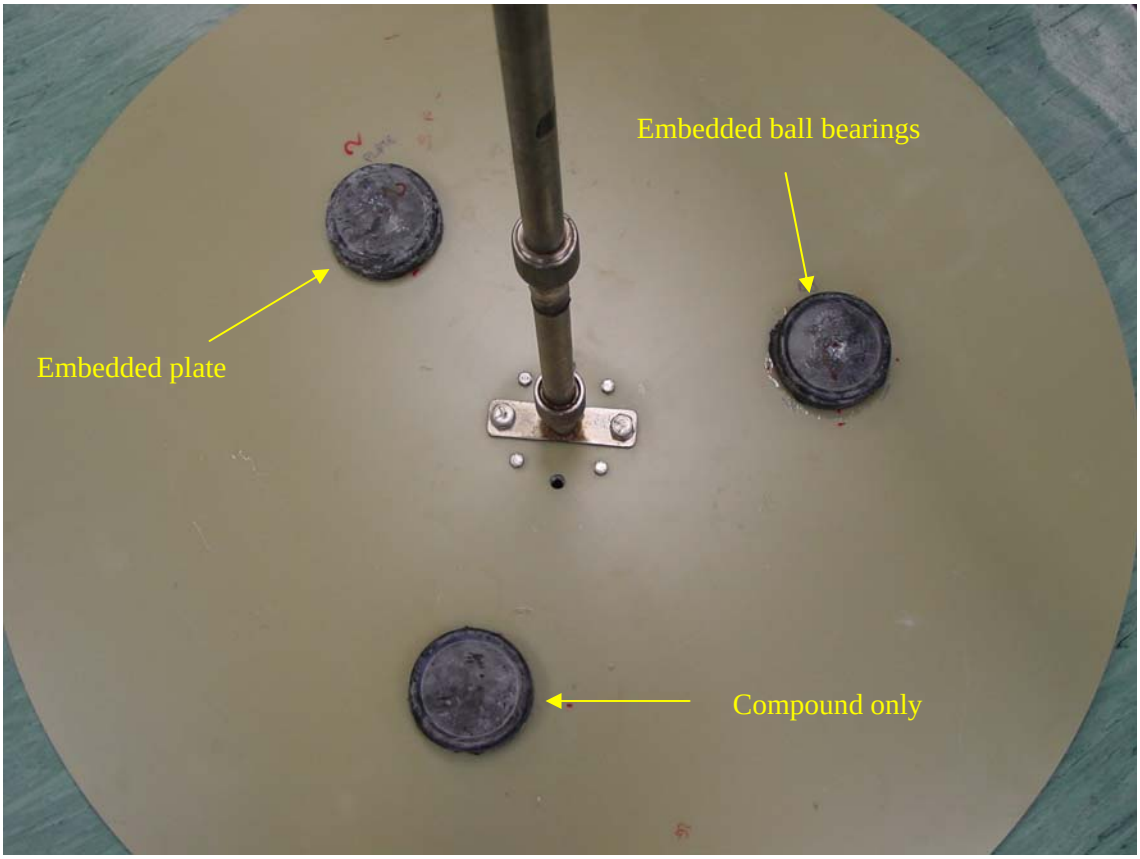

Figure 13 Top view of all three mineshapes mounted on the fibreglass disc.

Figure 14 Mineshape with embedded steel ball bearings.

Figure 15 Ball bearing-embedded mineshape atop polymer-bodied practice limpet mine.

2.2.3 Other targets

A 4cm diameter tungsten carbide sphere and an aluminum disc (1.64 cm thick and 15.3 cm in diameter) were also employed as targets in some of the measurements (see Figures 16 and 17).

Figure 18 shows a typical measurement set-up where the polymer-bodied and right cylindrical practice limpet mines are installed on the 1 metre diameter aluminum mounting disc and the HFMMPP/hydrophone are in bistatic configuration.

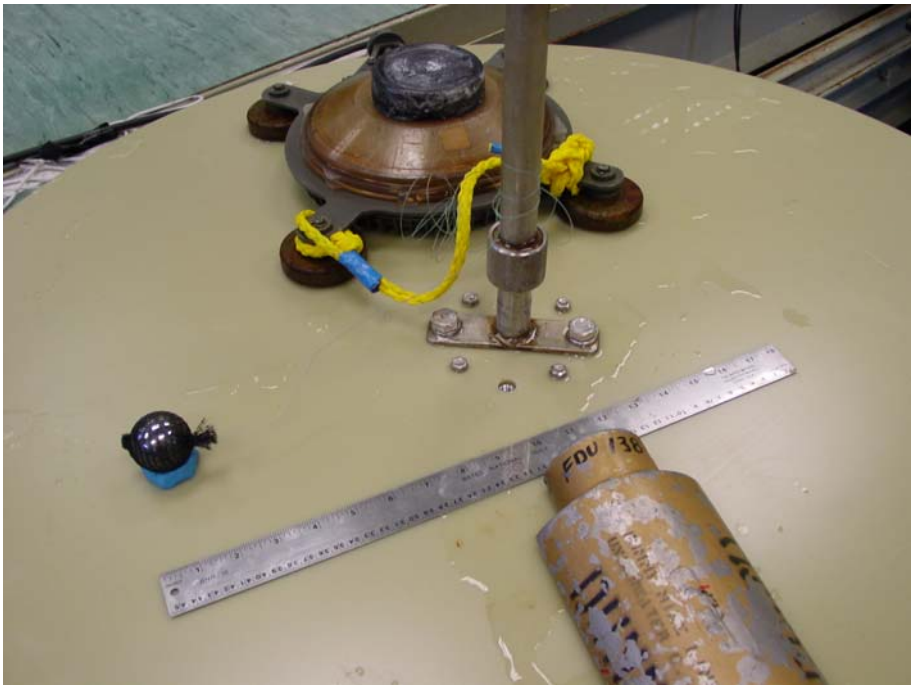

Figure 16 Tungsten-carbide sphere mounted on fibreglass disc with polymer-bodied and right cylindrical practice limpet mines.

Figure 17 Aluminum disc target and hemispherical practice limpet mine on fibreglass disc.

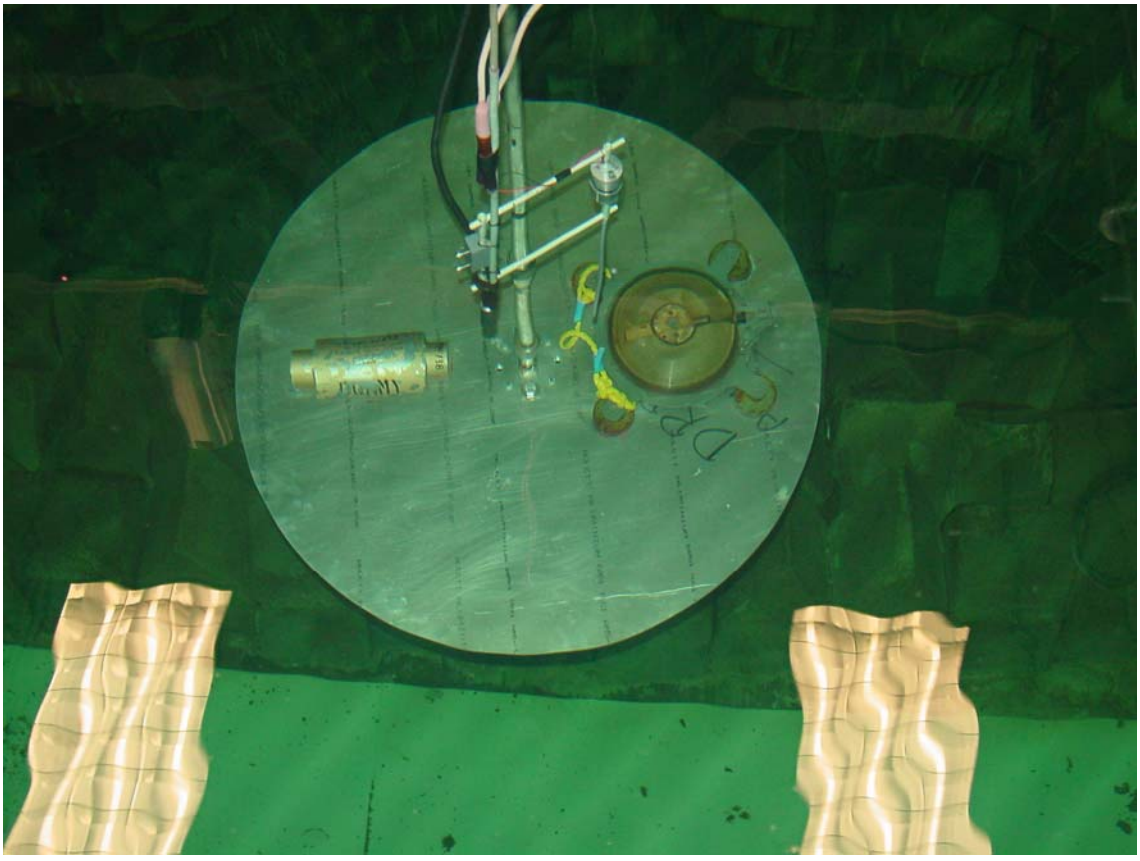

Figure 18 Bistatic ensonification of the polymer-bodied and right-cylindrical practice limpet mines mounted on the 1m aluminum disc.

3 Experimental Results

A variety of incident pulses are considered in this report: a [17 57] kHz compensated Sinc pulse, an uncompensated [8 90] kHz Sinc pulse, and compensated [9 103] and [50 110] kHz pulses. The term "Sinc" denotes that the spectrum of the specified waveform to the projector is unity across the frequency band. However, due to the transfer function of the projector, the spectrum of the output pulse in the water will not be flat. A compensated pulse signifies that the waveform input to the HF MMPP projector is specified so that the resulting output spectrum from the projector is unity across the band. The method for computing such an input waveform is described in Ref.1. For the uncompensated pulse, the input waveform had a flat spectrum in the [8 90] kHz band and we simply used the resulting output pulse as the incident pulse. We tried to construct a compensated version of this pulse but the result seemed to produce very poor results when used for scattering from the plate. The reasons for this are not clear – perhaps there were some non-linear effects in causing either the hydrophone or plate to vibrate. Later in the experiments, the projector/receiver setup was changed to that of Fig.3. In this configuration, it was possible to use higher frequency wideband compensated pulses and we used [9 103] and [50 110] kHz compensated pulses. Overall, using the two types of plates, different sets of objects, different HF MMPP and receiver configurations, and different incident pulses, we carried out 34 rotations.

The 2 incident pulses [17 57] kHz (compensated) and [8 90] kHz (uncompensated) and the echoes from the aluminum plate (40 cm from hydrophone) are shown in the time series of Fig.19. The reflections from the aluminum and fibreglass plates appear to be visually similar. In Figs. 20 and 21 we show some two-dimensional plots of the reflected time series as a function of the ping number for entire rotation of the plates, first the aluminum plate and then the fibreglass plate. In both cases, the larger polymer-bodied practice limpet mine is encountered first and then the smaller right-cylindrical unit. The bandwidths of the incident pulses and the distances of the hydrophone to the plates are indicated in the figures. The two objects are easily observed. Also, the diffractions from the objects can be seen in the echoes for sometime before and after the object is actually under the projector. This is due to the objects' scattering characteristics but also because the projector has a significant beamwidth (particularly at lower frequencies) and the hydrophone is omnidirectional. It can also be seen that the plate echo is not flat as a function of time, indicating that the rotation was somewhat skewed. This was subsequently verified by observing a red laser spot on the edge of the plate as it was rotated. The reflections from the upper shell of the objects are easily distinguishable and their arrival time relative to the plate yields a very good estimate of their height. There is some evidence of additional scattering from within the objects; however, it is difficult to distinguish this from the background plate reflection. Despite the fact, that the object blocks the acoustic energy from directly reaching the plate behind the object, there is off-axis energy and perhaps diffracted energy from the object which will reach the plate to the side of the object and scatter back to the receiver. Thus, for the smaller right-cylindrical unit, it can be seen that the reflection from the plate seems to continue "under" the reflection from this object. However, there is a slight delay in arrival time with respect to the surrounding plate arrivals.

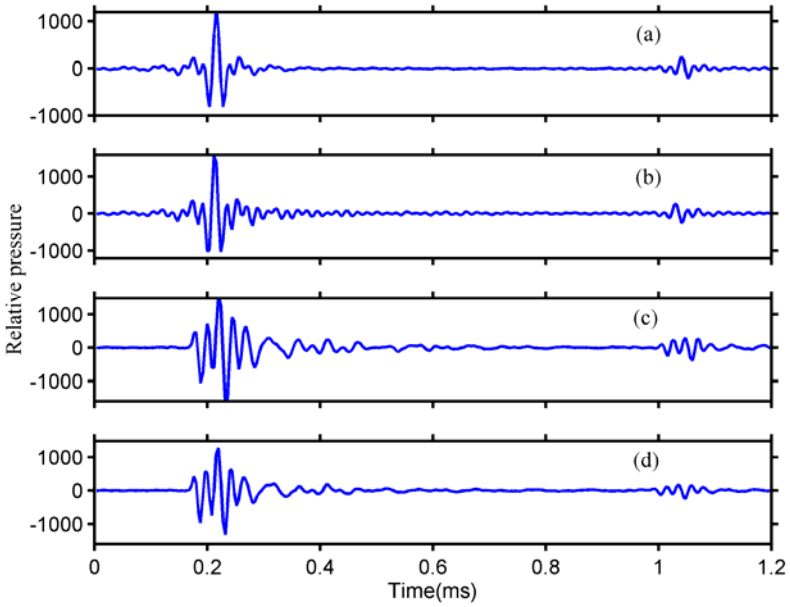

Figure 19 Four recorded echoes for the (a) compensated [17 57] kHz pulse above aluminum plate, (b) compensated pulse above fibreglass plate, (c) uncompensated [8 90] kHz pulse above aluminum plate, and (d) uncompensated pulse above fibreglass plate. The hydrophone/plate offset is 60 cm.

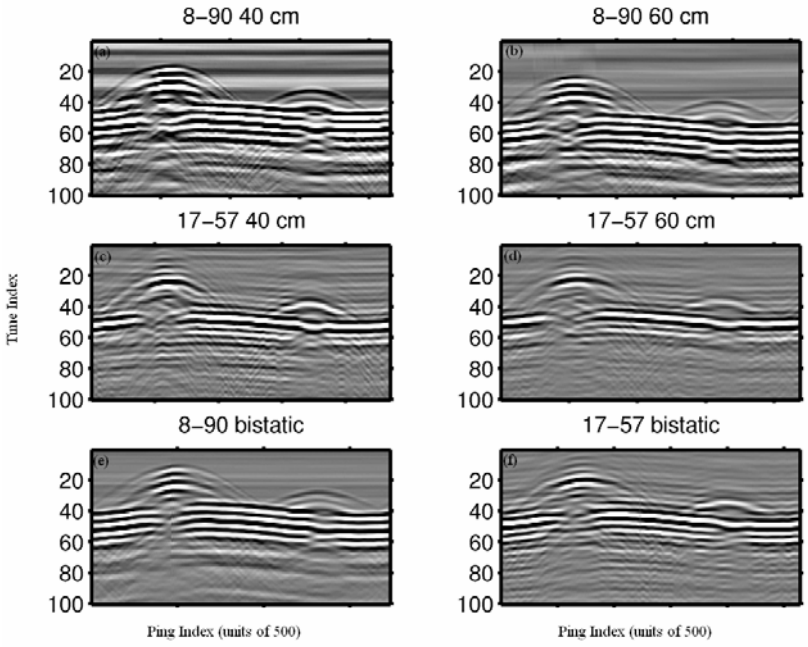

Figure 20 Time series as a function of ping number for the various pulse types and distances for the aluminum plate. Black represents negative pressure and white are positive values. The first target is the polymer-bodied practice mine and the second is the small right cylindrical mine.

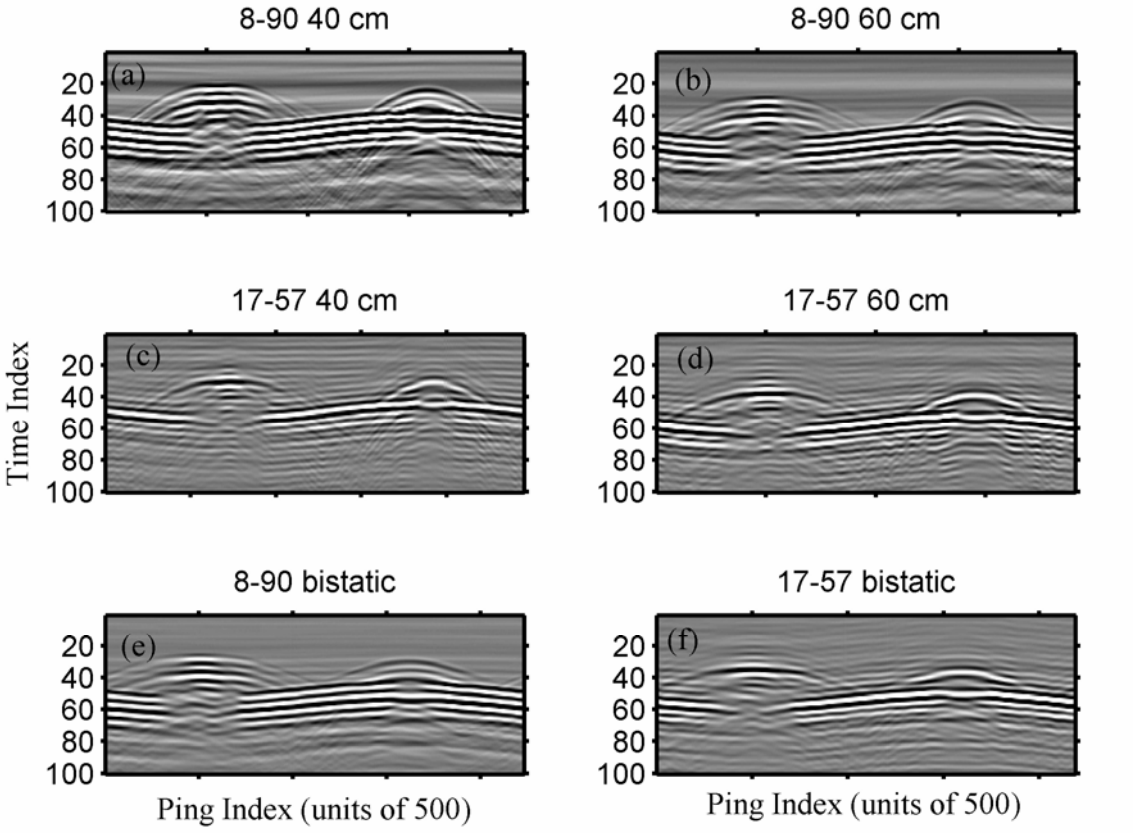

Figure 21 The same experimental setup as the previous figure but using the fibreglass plate.

In Fig.22 we show some miscellaneous results for the fibreglass plate. For some of the rotations we changed the target set. We placed the small mine-like target of Ref.1 on the top of the polymer-bodied limpet mine (see Figure 15); this object which contains a mixture of epoxy and small steel ball bearings acts as an attenuator. The right-cylindrical practice limpet mine was as before. In addition, we placed a small tungsten-carbide sphere between the 2 larger targets. Due to the beamwidth of the source and receiver, this sphere is not observable as a distinct entity. For the next 4 plots, (c)-(f), the projector/hydrophone arrangement of Fig.3 was used. In the second 2 plots (c) and (d), we consider a third limpet mine, an aluminum-shelled hemispherical target and a small aluminum disc. This disc is small but gives a strong and observable reflection near the start of the rotation. The hemispherical mine gives a weak return and also blocks out much of the plate return. There is some evidence of internal scattering, particularly for the [17 57] kHz pulse. Finally, the last 2 plots are for the original mineshapes; polymer-bodied and right-cylindrical. A [17 57] compensated sinc pulse is used as before and also a higher frequency [50 110] kHz pulse. It was found the natural response of the system in this frequency band was, in fact, quite flat and the compensation did not result in a significant loss of amplitude. It seemed that the higher frequencies accentuated an observed internal scattering event in the right-cylindrical shape.

We will now examine, in more detail, the time series and Fourier spectra for some representative echoes. We start by considering the plate-only (or as isolated as we can get from the targets)

echoes for the aluminum and fibreglass plates. In Fig.23 we show the echoes from the aluminum and the fibreglass plates, superimposed upon each other. The ping time series were normalized in both cases to have maximum amplitudes of unity (which corresponded to the incident pulse). As can be seen, the plate echoes are almost identical for the 2 cases. There are small differences at the end of the echo, but these differences are probably not sufficiently large with respect to the variation between pings and variations in the incident pulse from one rotation to another to consistently differentiate the 2 plates. A comparison of the incident pulse and the echo (Fig.24) for one of the pings (fibreglass) shows that the echo is not a simple reflected copy of the incident pulse. It should be noted that it is difficult to determine the exact mechanism for the plate echo. There is the echo from the tine plate itself, surrounded on both sides by water. There is also the fact that the disc of material is finite and that various global plate modes may be induced by the incident energy.

In figures 25 to 28, we show the time series and corresponding spectra of the incident-, plate- and target-reflected pulses. These correspond to a variety of different pulse shapes and targets. In Fig.25 we show some time series from rotations 10 and 22, which correspond to Fig. 20d and Fig.22b. The left column shows the incident pulse portion of one of the time series from the rotation, the middle column shows a representative echo from the plate from one of the time series, and the third column shows extracted echoes from selected time series. The first row shows the echo from the flank of the polymer-bodied mine, the second directly over top of this shape. The third plot is directly over the right-cylindrical shape. The fourth plot is from another rotation, this time using the fibreglass plate, and over the polymer-bodied mine with the ball bearing-impregnated, rubber compound mineshape on the top. The echoes have been normalized so that their maximum absolute value is unity. Within the 101-point window, it can be seen that the echoes are quite different in character from the incident or plate echoes. In particular, notice the phase inversion of the incident pulse as a result of the reflection from the polymer-bodied mine. The echo from the right-cylindrical mine consists of a “rigid” reflection (i.e., the polarity is the same as the incident pulse) followed by the plate echo. In Fig.26, we show the Fourier Spectra corresponding to the time series of Fig.25. The first and third echoes have a spectrum with “peaks” and “troughs”. The second and fourth echoes have a flatter spectrum with a peak at about 50 kHz, which maybe partly due to noise.

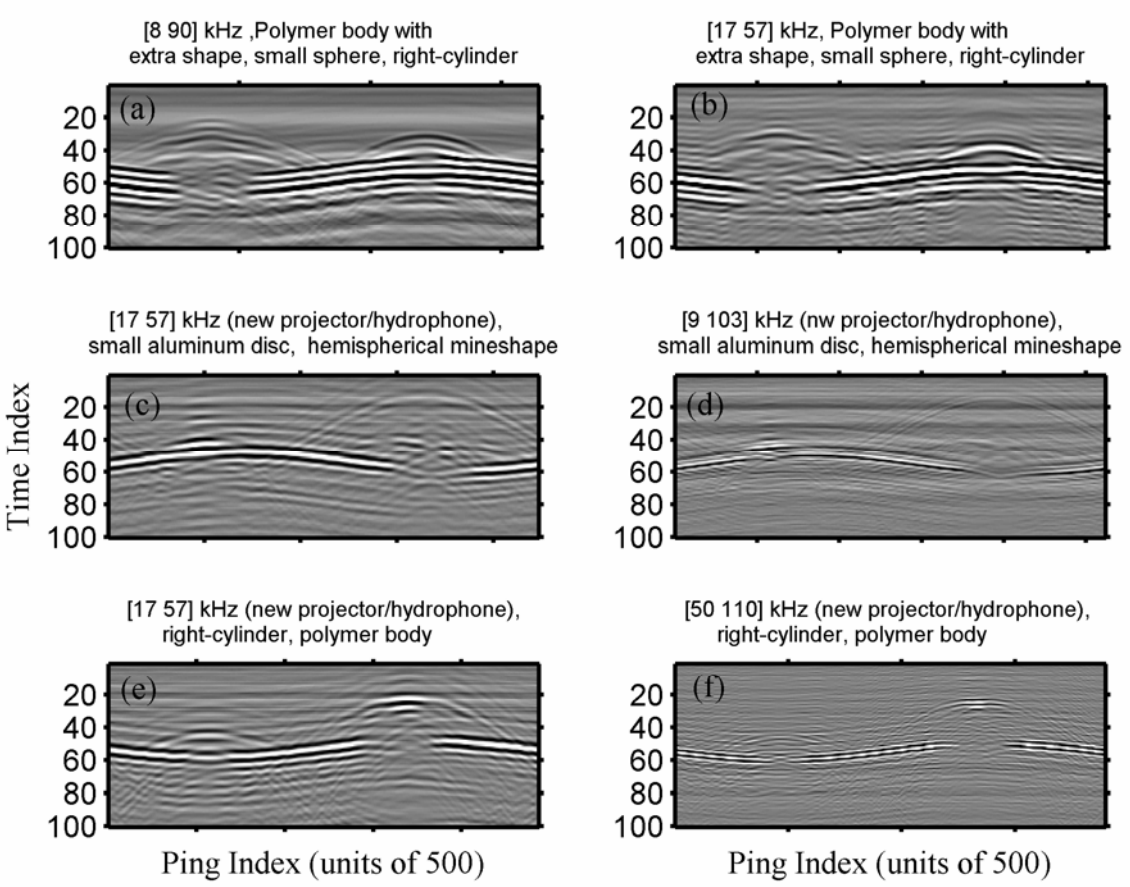

Figure 22 The time series for (i) top 2 plots, the polymer-bodied practice limpet mine with an additional ball bearing- impregnated rubber mineshape on top, small tungsten carbide sphere and right-cylinder (ii) the middle 2 plots, show 2 new targets, a small aluminum disc and a hemispherical mine, (iii) the polymer-bodied and small right-cylindrical mine. The last 4 plots use the new projector/hydrophone arrangement.

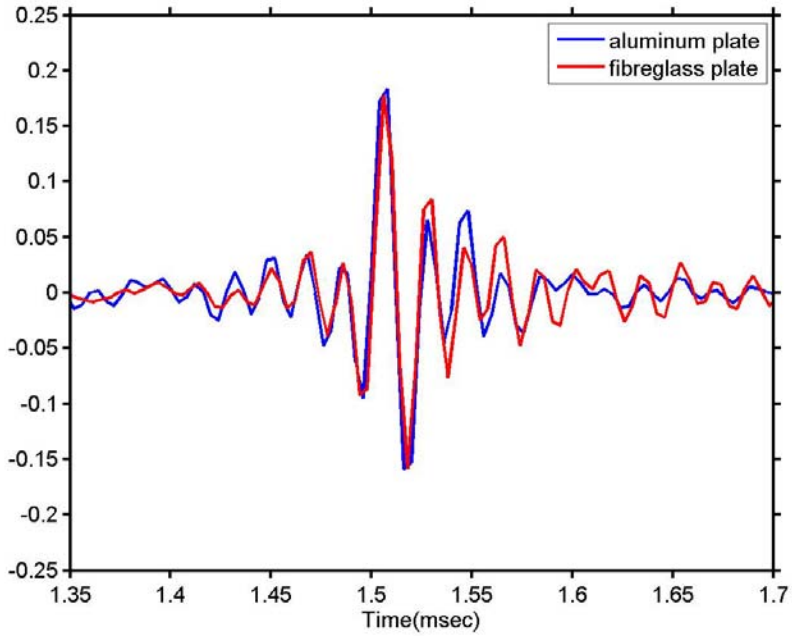

Figure 23 A comparison of the echoes from the 2 types of plate. The incident pulse was the [17 57] kHz compensated pulse at a hydrophone distance of 60 cm. The first projector/hydrophone arrangement was used.

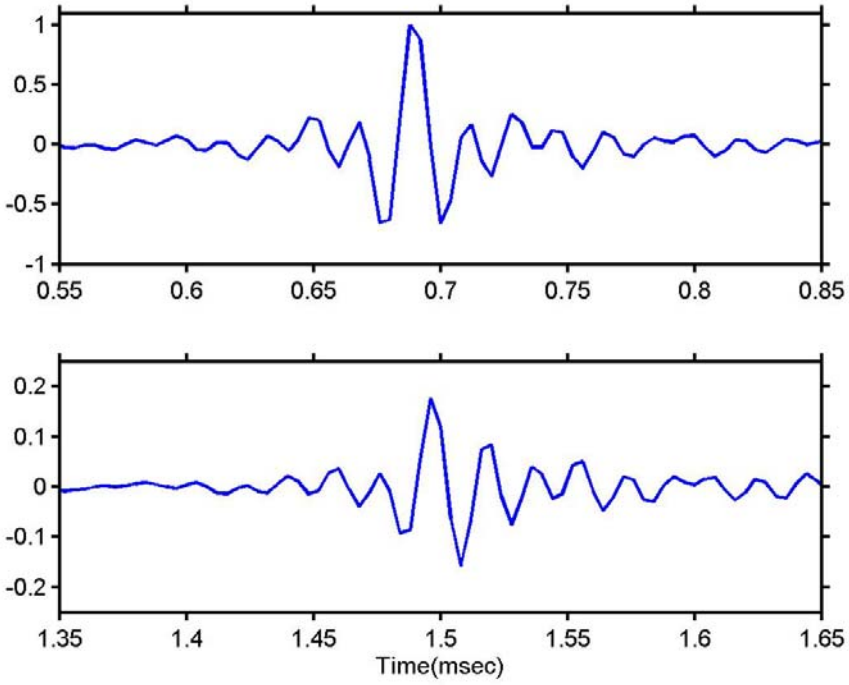

Figure 24 The direct and plate-reflected echoes for the fibreglass plate, [17 57] kHz incident pulse.

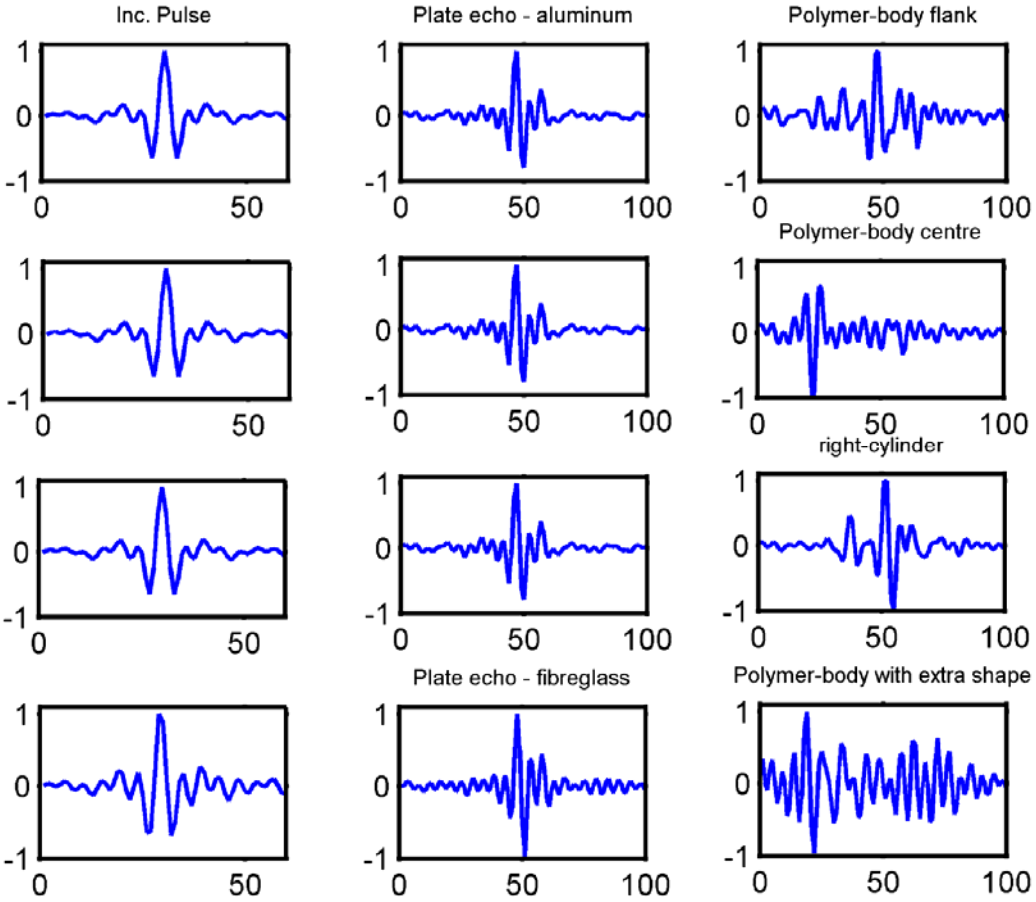

Figure 25 Some representative, incident pulses, plate echoes and targets echoes for top row: flank of polymer-bodied mine, second row, over top of polymer-bodied mine, third row, over right-cylindrical mine and fourth row, over polymer-bodied mine with extra absorbing mineshape. A compensated [17 57] kHz pulse is used for all these cases with the first projector/hydrophone arrangement. The top3 figures are for the aluminum plate and the last row is for the fibreglass plate.

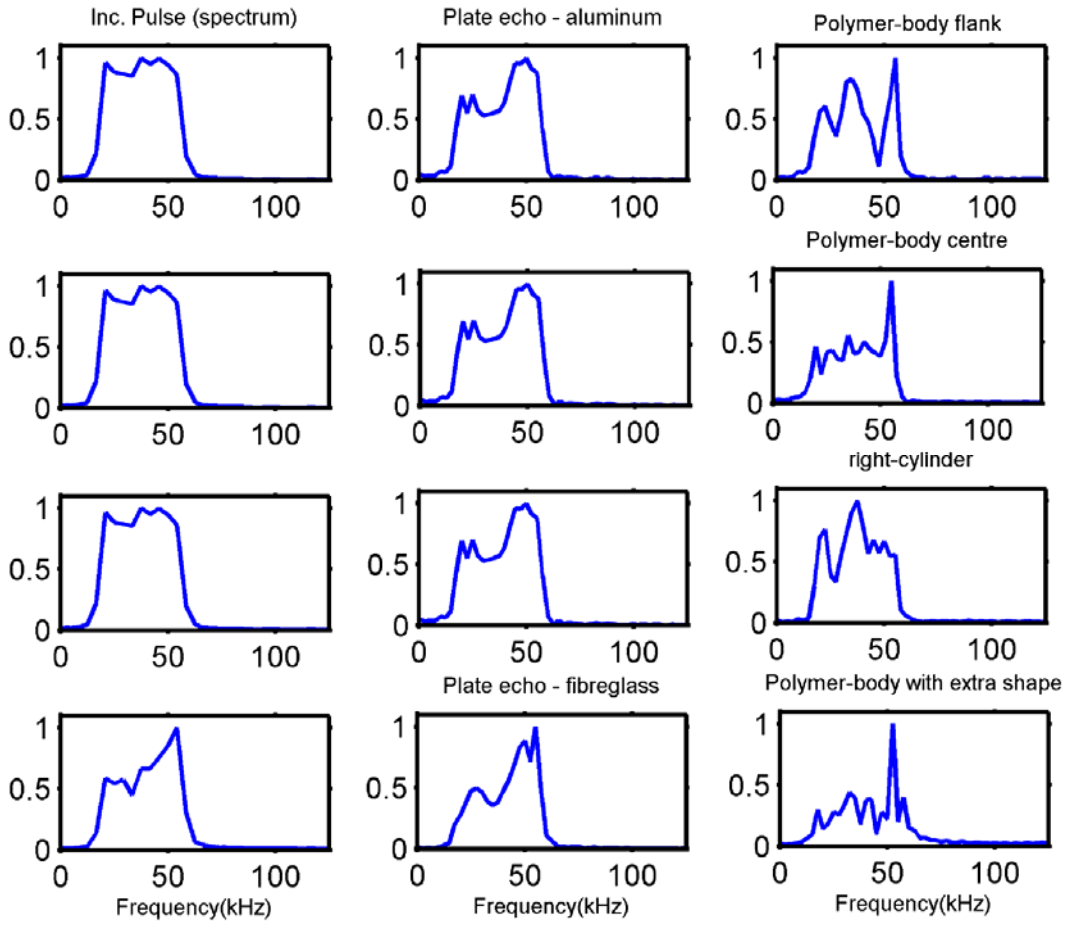

Figure 26 The Fourier spectra corresponding to the time series of Fig.25.

In Figs. 27 and 28 we show some more echoes and their spectra. The first 2 plots are for the [17 57] kHz compensated pulse over the fibreglass plate. The targets are the small aluminum disc and the hemispherical mine (Fig.22c). The second 2 plots are for a [50 110] kHz compensated pulse, over the fibreglass plate, with the polymer-bodied mine (corresponding to Fig.22e). The second projector/hydrophone arrangement was used for these measurements. In this case, the echoes from the plate and the targets were a little more in the tail of the incident pulse than in the previous arrangement. However, it can be seen that the target echoes are distinctive relative to the plate echo. For the [50 110] kHz pulse, the small right-cylindrical mine has quite a strong response. For the polymer-bodied mine, the echo is once again approximately a phase-inverted version of the incident pulse. The corresponding spectra are shown in Fig.27. With the exception of the phase-inverted echo from the polymer-bodied mine, one can see that the spectra of the echoes are quite different than those of the incident pulse or plate echo.

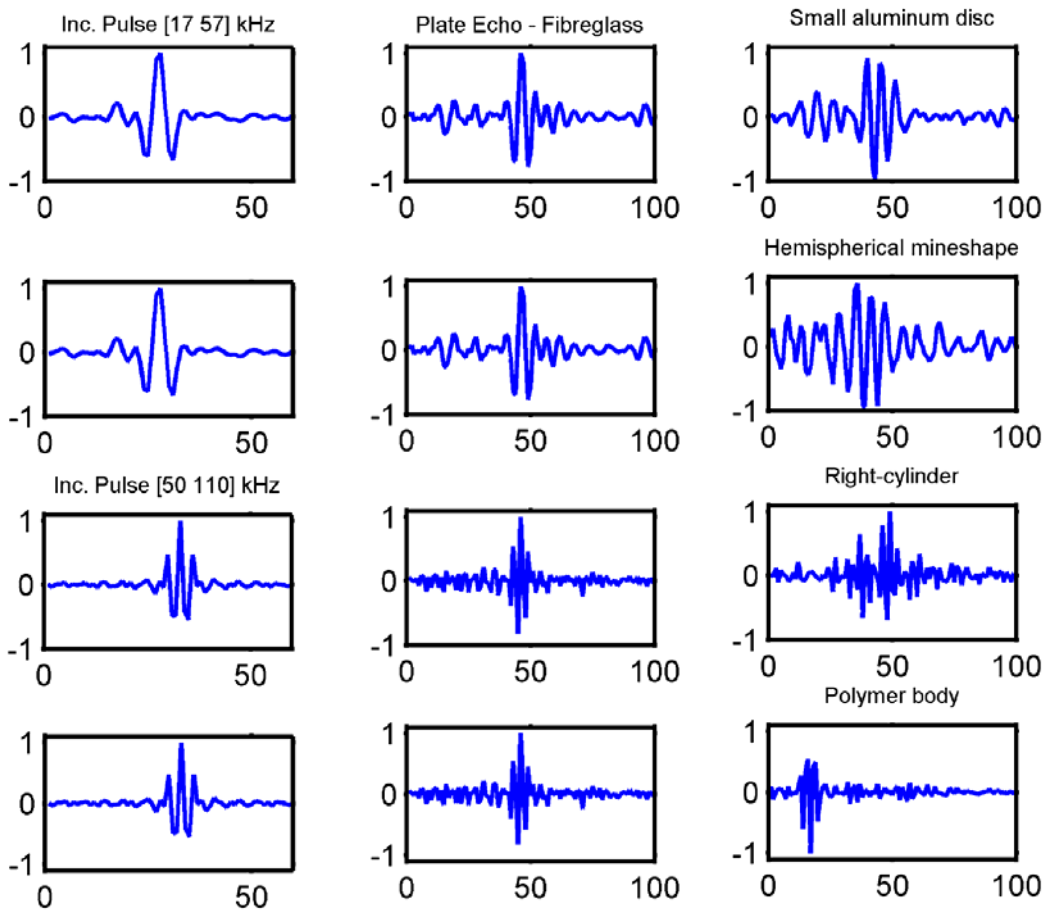

Figure 27 Some representative time series. The first 2 rows show the [17 57] kHz pulse and the echoes from the small aluminum disc and then the hemispherical mines. The last 2rows show the [50 110] kHz pulse over the small right-cylindrical and polymer-bodied mines. These results are for the second projector/hydrophone arrangement.

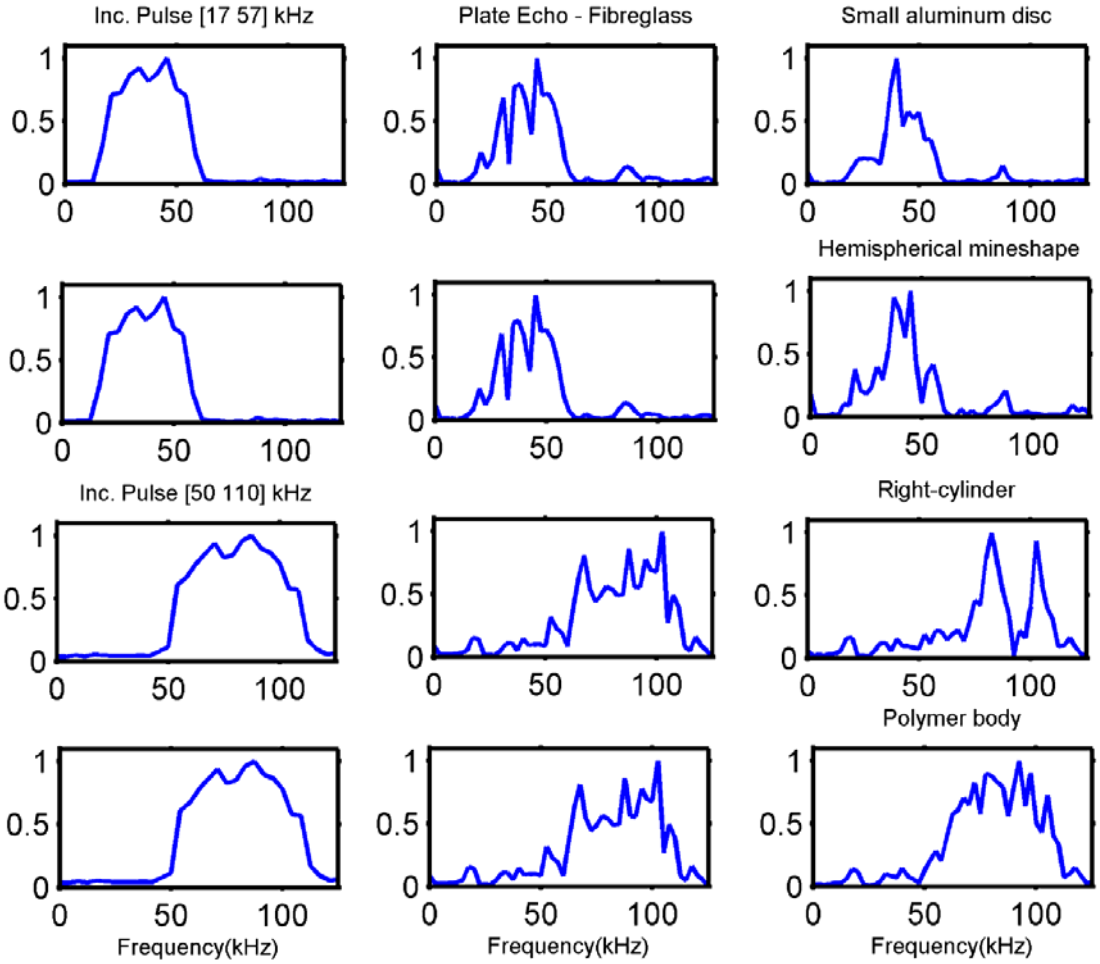

Figure 28 Some representative spectra. The first 2 rows show the [17 57] kHz pulse and the echoes from the small aluminum disc and then the hemispherical mine. The last 2 rows show the [50 110] kHz pulse over the small right-cylindrical and polymer-bodied mines. These results are for the second projector/hydrophone arrangement.

As a final set of rotations, we consider the 3 ad hoc mineshapes based upon the shape of Ref.3 and a molded rubber compound (Fig.13). There is no difference between the shapes; however, in the interior of one of the shapes there is an aluminum disc which approximately occupies about 12% of the interior volume. The second shape consists just of the epoxy material and the third shape consists of the epoxy and small steel ball bearings. In Fig.29 we show the time history of the echoes for 3 different incident pulses: [17 57] kHz, [9 103] kHz, and [50 110] kHz. The reflection from the shape with the aluminum disc is quite evident for all 3 pulse types. The reflections from the other 2 targets are weaker and these targets are somewhat characterized by a lack of a strong echo. The 3 targets seem to be most evident for the wideband pulse [9 103] kHz, Fig.29b. In Figs.30 and 31, we show some of the time series and corresponding spectra in detail for the [9 103] kHz pulse. The aluminum disc causes quite a strong reflection (even though the

disc is contained within the mineshape) followed by a second reflection. The mineshape with just the rubber compound produced a weaker reflection (recall that the time series in Fig.30 have been normalized to have a maximum absolute value of unity) but the echo is quite distinctive. The shape with the rubber compound and the ball bearings is perhaps the most difficult to visually distinguish from the plate echo although there are differences. These differences are also observed in the normalized spectra of Fig.31. The last 2 spectra have relatively more energy in the lower frequency band than the plate echo. For the unnormalized spectra, the higher-frequency content of these target echoes is smaller because of the attenuating effect of the rubber compound.

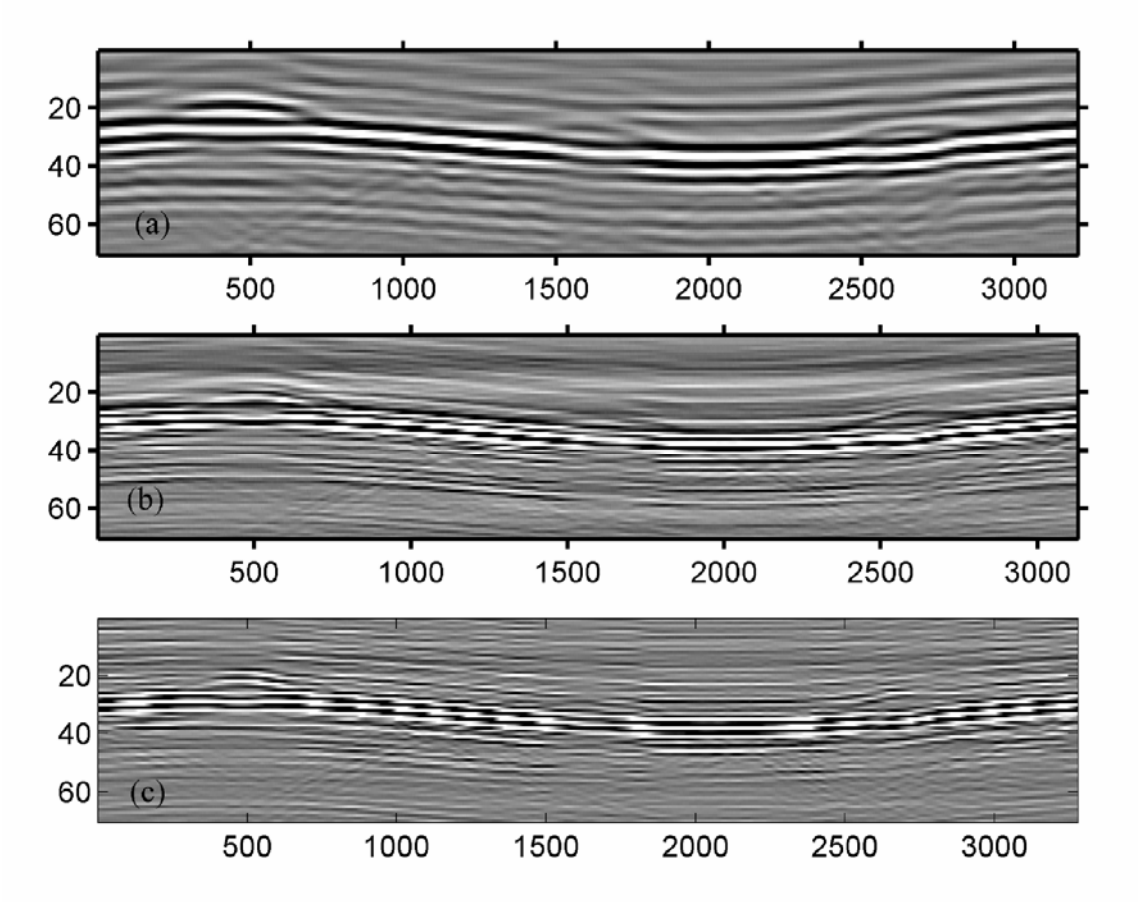

Figure 29 The rotation time series for the 3 rubber compound mineshapes using [17 57] kHz, [9 103] kHz and [50 110] kHz pulses

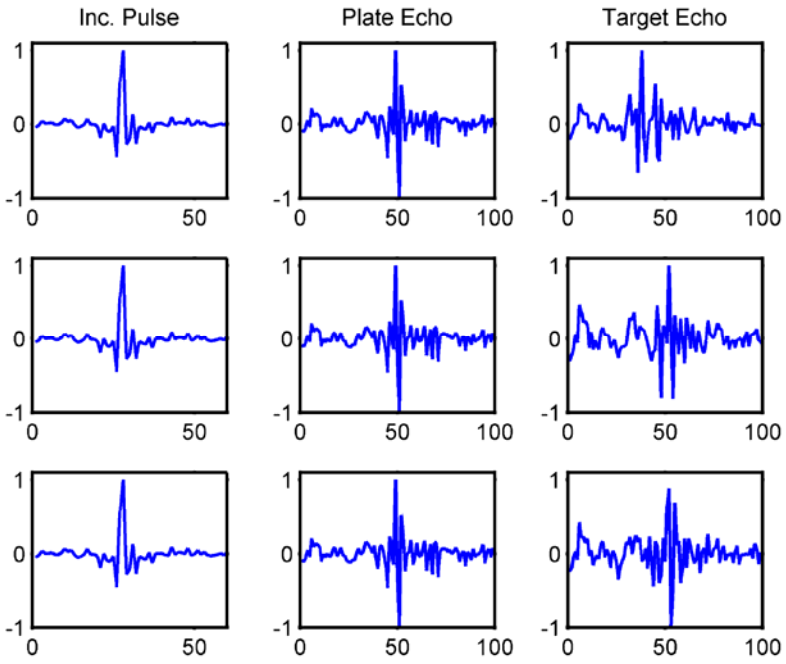

Figure 30 The incident, plate echo and target echoes for 3 identical mineshapes with: [top] rubber compound-fill and interior aluminum disc, [middle] rubber compound-fill only, and [bottom] rubber compound-fill with steel ball bearings. The incident pulse is the compensated [9 103] kHz pulse.

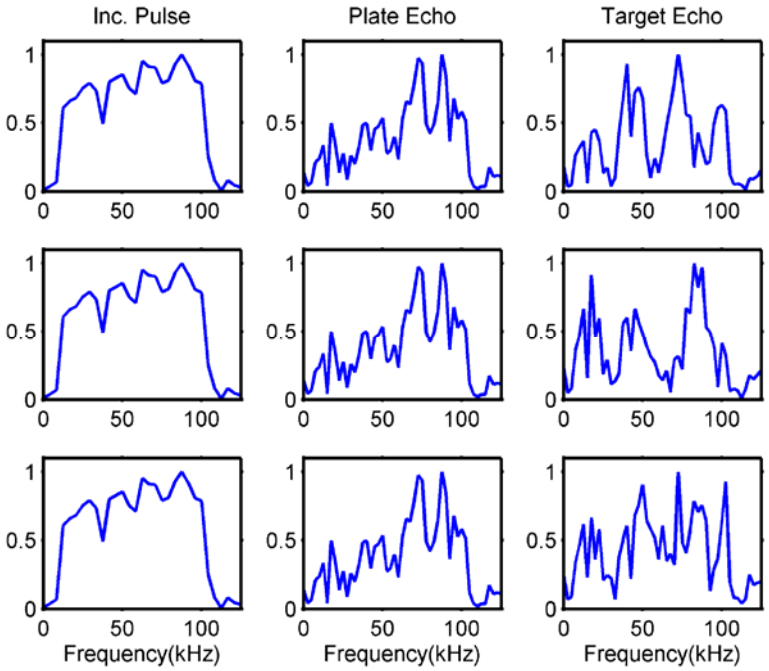

Figure 31 The spectra corresponding to the time series of Fig.30.

4 Change Detection and Classification

In the previous sections, we have presented many time series and Fourier spectra which have illustrated that the target echoes are distinguishable from the background plate response. The example of the aluminum disc within the rubber compound mineshape indicated that energy can penetrate into the mineshape and reflect from internal structure. In this section, we first consider the automated detection of changes from the background plate echo. We will do this on the basis of the cross-correlation of the time series with the plate echo (in particular, the change as the targets are approached) and on the basis of the normalized difference of their spectra. In both these approaches, the actual amplitude of the return is not utilized. Second, we will consider a traditional training and testing classification study for multi-class classification. For the first example, we consider the rotation of the aluminum plate, at 60 cm distance from the hydrophone, using the [17 57] kHz pulse with first the polymer-bodied practice limpet mine and then the small right-cylindrical mine (this corresponds to Fig.21d). We selected one 101-point time series as representative of the plate echo and normalize this to have unity norm. We then consider the same time window, which is large enough to include the plate and target echoes from the entire rotation. We cross-correlate each of these time series (normalized) with the reference plate echo. We then consider the maximum absolute value of the envelope of this cross-correlation multiplied by the sign of the cross-correlation at this point. The use of the sign is to distinguish the case of the pulses being phase-reversed, which is the case for the polymer-bodied mine. The resulting output is shown in Fig.32. The polymer-bodied mine is very evident (because of the change in sign) and the right-cylindrical mine is also observable just after ping 1500. It is interesting to note that the gradual decrease in correlation as the targets are approached. We can also consider the spectrum (the absolute values) of the reference plate echo normalized to have unity norm. This spectrum is then compared to the normalized spectra (absolute values) of the echoes as the plate is rotated; the absolute value of the sum of differences is computed. The resulting output is shown in Fig.33. In this case, it is the small right cylindrical mine target which is more easily observable. Using a combination of the cross-correlation and the spectral differences should lead to an even more powerful detection method. In Figs.34 and 35, we show the same types of output for the rotation with the [9 103] kHz pulse involving the 3 identical rubber-compound mineshapes (but different internal structure). In this case, the representative plate echo timeseries was ping 2050 and was taken from a region between the second and third mineshapes where the plate appeared flat in the rotation time series. However, unlike the results of Fig.32, where the correlation of the plate echoes with the representative plate echo was above 0.9 (except near the targets), it can be seen that in Fig.34 the correlation of the plate echoes with the representative time series is sometimes less in this case. However, the rubber compound mineshape with the internal aluminum disc is readily identifiable on the basis of the timeseries cross-correlations. The mineshape, with just the rubber compound-fill is also easily identifiable. The mineshape with the rubber compound and ball bearings is barely identifiable. On the basis of the spectral differences, Fig.35, all 3 targets are readily observed.

In the previous examples, we considered the detection of the target regions on the basis of a change from the surrounding background response. In the next set of examples, we consider the multiclass classification problem where we attempt to classify specific object types. Once again, we consider the [9 103] kHz pulse. We define the intervals of the rotation ping sequence, Fig.29b, corresponding to echoes from the 3 targets and the remainder of the ping history is defined as the

plate. Three features based upon the time series and spectra: (1) the ratio of the sum of the absolute values of the spectra in the band [50 125] kHz to the sum of the absolute values in [10 35] kHz. (2) the ratio of the standard deviation squared of the time series to the mean absolute value squared (3) the maximum absolute value of the envelope of the cross-correlation between the echo and a reference plate echo are computed. The distribution of these feature values for the 4 possible classes: target 1 (with interior aluminum disc), target 2, target 3, and the plate are shown in Fig.36. For each of the 4 classes, we take ¼ of the pings and their associated features as a training database and the remainder as the testing set. The target classes (red, green, and yellow) are for the most part clearly separable from the plate features. Also, when defining the ping intervals for the targets, there are pings near these ping boundaries which appear as blue in Fig.36. The resulting classification of the ping history (testing set) is shown in Fig.37 using a nearest-neighbour classifier. As can be seen, the sequence of classifications is very good.

As in Ref.3, we can also use the normalized FFT spectra as the features. We once again use a random 25% of the pings of each class for the training set and the remainder in the testing set. In this case we perform the random partitioning 21 times and compute an averaged Confusion matrix which is shown in Fig.38. As can be seen, the classification performance is almost perfect with all diagonal elements greater than 98.5%.

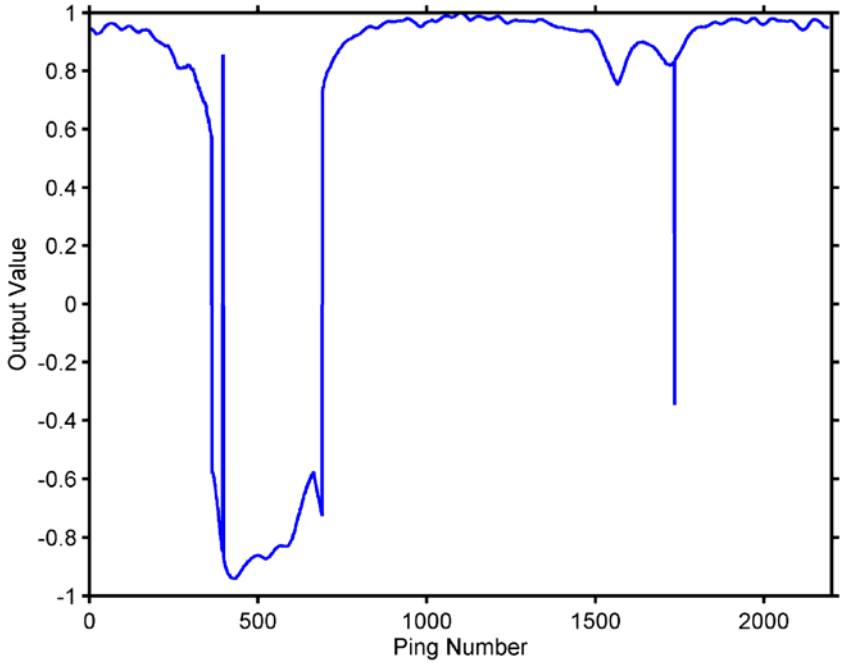

Figure 32 The cross-correlations (described in the text) of the echo time series with a reference plate echo. The first target is the polymer-bodied mine and the second is the small right-cylinder mine (see Fig.20d) for the [17 57] kHz compensated pulse.

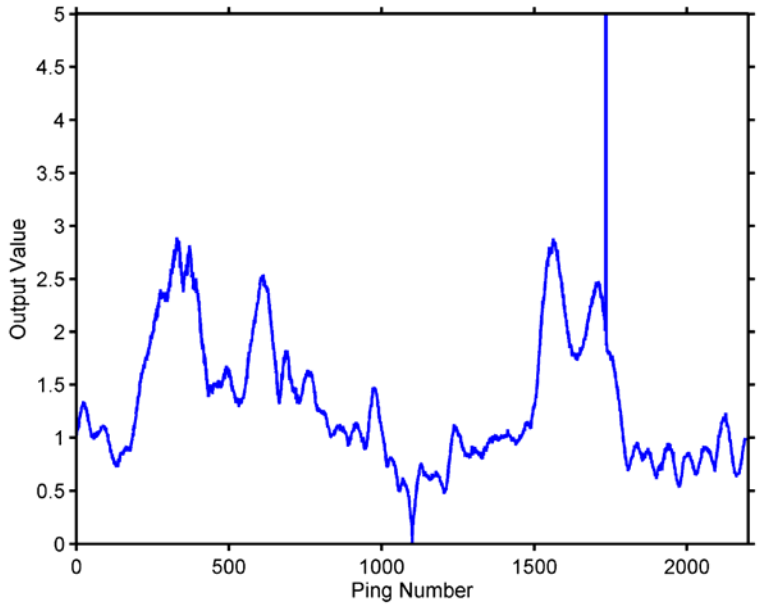

Figure 33 The differences between echo spectra (absolute values) and reference plate spectra. . The first target is the polymer-bodied mine and the second is the small right-cylinder mine (see Fig.20d) for the [17 57] kHz compensated pulse.

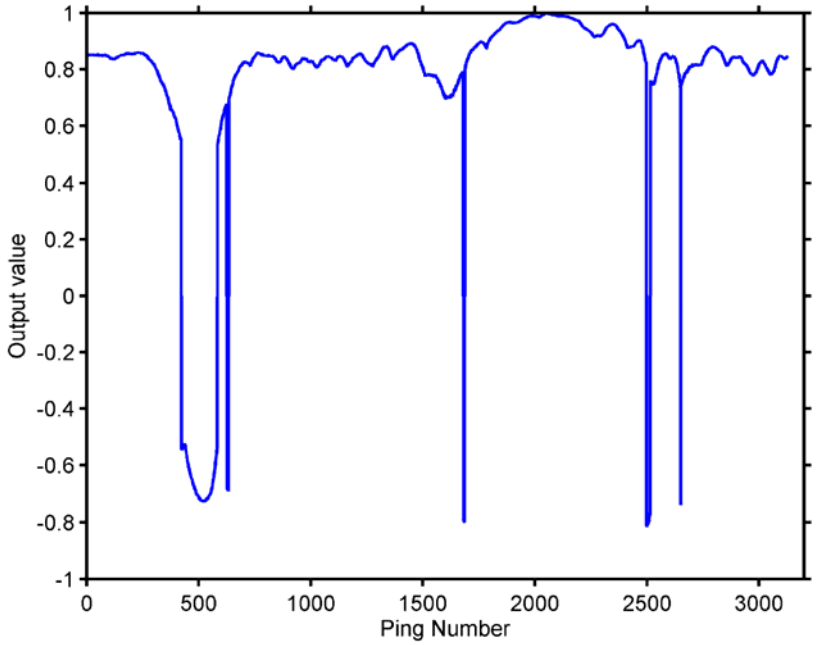

Figure 34 The cross-correlations between the echo timeseries and the reference plate time series for the 3 identical rubber compound mineshapes of Fig.29b ([9 103] kHz pulse)

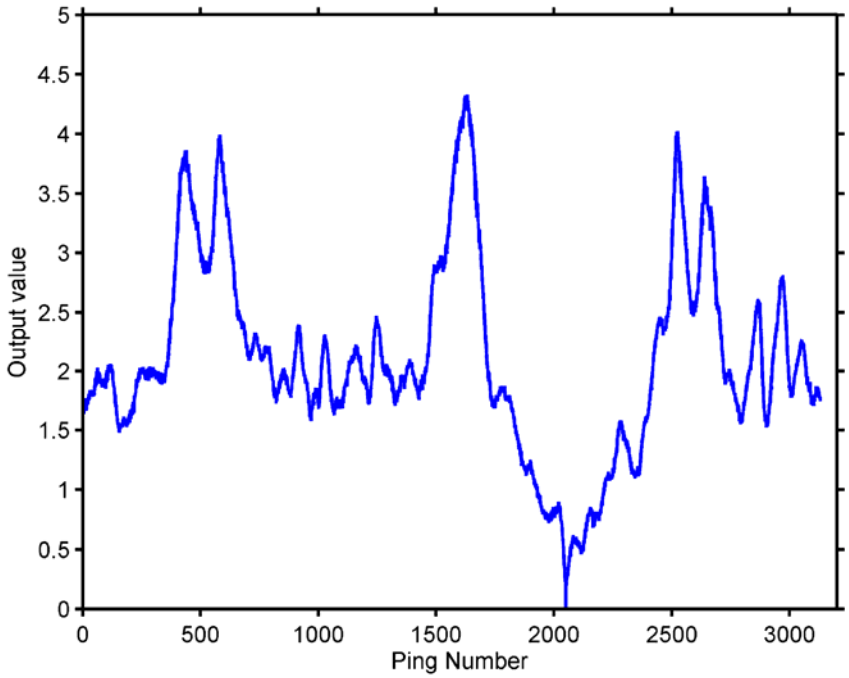

Figure 35 The differences between the echo spectra and the reference plate spectrum for the 3 identical rubber compound mineshapes of Fig.29b ([9 103] kHz pulse)

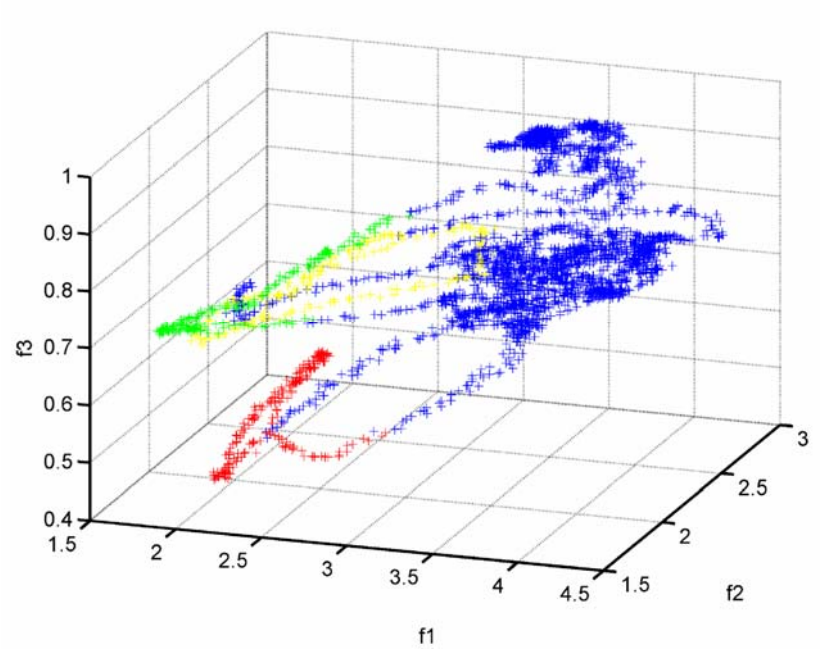

Figure 36 The distribution of the three features for the 4 classes; target 1 (red), target 2 (green), target 3, (yellow) and plate (blue)

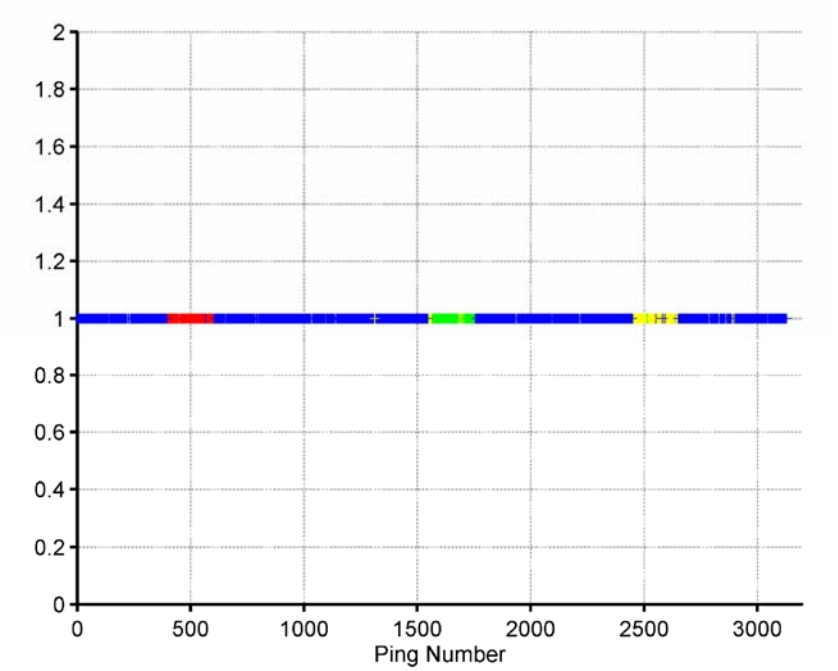

Figure 37 The resulting classifications of the pings of the testing set using 3 features and a nearest neighbour classifier with a training set.

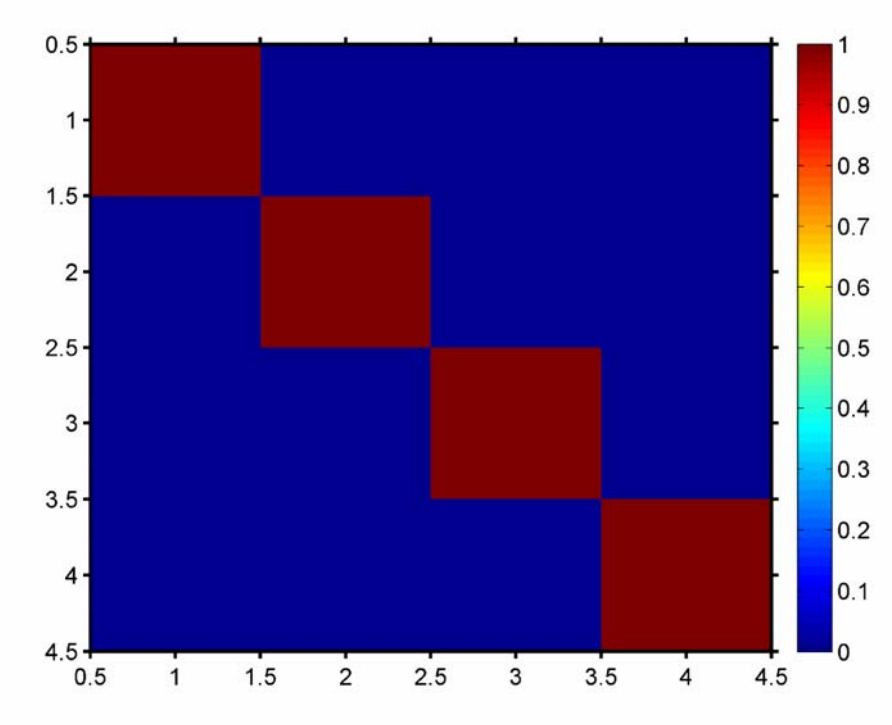

Figure 38 Resulting Confusion matrix from using the FFT spectra (absolute value, and normalized) and nearest neighbour classifier.

5 Summary and Discussion of Results

We have shown that the echoes from a very broadband incident pulse can be used to discriminate objects of interest from other scattering objects or from background echoes coming from a surrounding plate. We considered 3 actual practice limpet mines and showed that they were clearly visibly distinguishable in the ping timeseries from the background plate echoes. The discriminating features include the arrival time of the leading echo which can yield estimates of the object's height, the amplitude of the target echo and the plate echo which may still appear later, and also the structure of the echo, both temporally and in the spectral domain. For example, the leading echo from the polymer-bodied mine showed a definite phase reversal from the incident pulse. We also constructed three identical rubber compound "mineshapes" which varied only in terms of their internal properties. One of these targets included a small aluminum disc surrounded by the rubber compound material. Relatively strong reflections from this disc were observed indicating that the acoustic energy was able to penetrate into this object and reflect off the internal structure. We also showed that we could automatically distinguish targets from the background plate echoes on the basis of changes of the cross-correlation with a representative plate echo or a change in the spectrum. There may be ship's hull internal features such as ribs, bulkheads, etc., that give rise to distinct scattering characteristics which may be amenable to inclusion in the classification scheme. A variety of different pulse types and bandwidths were used. Depending upon the targets of interest and the background characteristics, certain frequency bands may be more important for the discrimination. The projector and the hydrophone used in the measurements had relatively large beamwidths (in the case of the HF MMPP projector, this is frequency-dependant with the beamwidth decreasing at high frequencies). We hope in the future to consider the beamforming of the data collected during this experiment.

Although, we considered targets which realistically simulated limpet mineshapes, they did not realistically simulate the internal explosive or for some of the shapes, the shell thickness. We would like to carry out even more realistic measurements in the future. In addition, we are hoping to integrate a HF MMPP/rectangular receive element system on a ROV so that more realistic ship or pier settings can be investigated.

References

[1] J. Fawcett, J. Sildam, T. Miller, R. Fleming and M. Trevorrow, Broadband Synthesis with the High Frequency Multi-Mode Pipe Projector, DRDC Atlantic Technical Memorandum, TM 2005-022 (2005).

[2] R. Fleming and J. Fawcett, Broadband pulse generation using bi-amplified MMPP's, DRDC Atlantic TM 2007-293 (2007).

[3] J. Fawcett and R. Fleming, Wideband detection and classification of practice limpet mines against various backgrounds, DRDC Atlantic Technical Memorandum, TM 2007-334 (2007).

List of symbols/abbreviations/acronyms/initialisms

DND	Department of National Defence
DRDC	Defence Research & Development Canada
DRDKIM	Director Research and Development Knowledge and Information Management
R&D	Research & Development
MMPP	Multi-mode pipe projector
HF MMPP	High frequency multi-mode pipe projector
ACT	Acoustic calibration tank
kHz	kilohertz

This page intentionally left blank.

Distribution list

Document No.: DRDC Atlantic TM 2008-079

LIST PART 1: Internal Distribution by Centre

1 John Fawcett
1 Richard Fleming
1 David Hopkin
1 David Hazen
1 Anna Crawford
5 DRDC Atlantic Library

11 TOTAL LIST PART 1

LIST PART 2: External Distribution by DRDKIM

1 Library and Archives Canada
1 DRDKIM

2 TOTAL LIST PART 2

13 TOTAL COPIES REQUIRED

This page intentionally left blank.

DOCUMENT CONTROL DATA

(Security classification of title, body of abstract and indexing annotation must be entered when the overall document is classified)

1. ORIGINATOR (The name and address of the organization preparing the document. Organizations for whom the document was prepared, e.g. Centre sponsoring a contractor's report, or tasking agency, are entered in section 8.)

Defence R&D Canada – Atlantic
9 Grove Street
P.O. Box 1012
Dartmouth, Nova Scotia B2Y 3Z7

2. SECURITY CLASSIFICATION (Overall security classification of the document including special warning terms if applicable.)

UNCLASSIFIED

3. TITLE (The complete document title as indicated on the title page. Its classification should be indicated by the appropriate abbreviation (S, C or U) in parentheses after the title.)

Wideband detection and classification of practice limpet mines against various backgrounds:

4. AUTHORS (last name, followed by initials – ranks, titles, etc. not to be used)

Fawcett J.; Fleming R.

5. DATE OF PUBLICATION (Month and year of publication of document.)	6a. NO. OF PAGES (Total containing information, including Annexes, Appendices, etc.)	6b. NO. OF REFS (Total cited in document.)
July 2008	50	3

7. DESCRIPTIVE NOTES (The category of the document, e.g. technical report, technical note or memorandum. If appropriate, enter the type of report, e.g. interim, progress, summary, annual or final. Give the inclusive dates when a specific reporting period is covered.)

Technical Memorandum

8. SPONSORING ACTIVITY (The name of the department project office or laboratory sponsoring the research and development – include address.)

Defence R&D Canada – Atlantic
9 Grove Street
P.O. Box 1012
Dartmouth, Nova Scotia B2Y 3Z7

9a. PROJECT OR GRANT NO. (If appropriate, the applicable research and development project or grant number under which the document was written. Please specify whether project or grant.)	9b. CONTRACT NO. (If appropriate, the applicable number under which the document was written.)
11cf	

10a. ORIGINATOR'S DOCUMENT NUMBER (The official document number by which the document is identified by the originating activity. This number must be unique to this document.)	10b. OTHER DOCUMENT NO(s). (Any other numbers which may be assigned this document either by the originator or by the sponsor.)
DRDC Atlantic TM 2008-079	

11. DOCUMENT AVAILABILITY (Any limitations on further dissemination of the document, other than those imposed by security classification.)
Unlimited

12. DOCUMENT ANNOUNCEMENT (Any limitation to the bibliographic announcement of this document. This will normally correspond to the Document Availability (11). However, where further distribution (beyond the audience specified in (11) is possible, a wider announcement audience may be selected.))

13. ABSTRACT (A brief and factual summary of the document. It may also appear elsewhere in the body of the document itself. It is highly desirable that the abstract of classified documents be unclassified. Each paragraph of the abstract shall begin with an indication of the security classification of the information in the paragraph (unless the document itself is unclassified) represented as (S), (C), (R), or (U). It is not necessary to include here abstracts in both official languages unless the text is bilingual.)

In this experiment we placed actual practice limpet mines on a one-metre diameter disc which was suspended in the DRDC Atlantic acoustic calibration tank from a rotator pole. Two different discs were considered: one, aluminum and the other fibreglass. These discs were then rotated under a fixed multi-mode pipe projector (MMPP) and hydrophone. The geometry was arranged so that the mineshapes would appear directly under the projector/hydrophone during the rotation. The measurements were made at 2 different disc-projector offsets and for a slightly bistatic arrangement. Various different incident pulses were considered corresponding to different frequency bands. It is shown that the mineshapes are often easily discriminated from the surrounding disc response, in terms of both the echo travel time and the characteristics (temporal and spectral) of the echoes.

Au cours de l'expérience, nous avons placé des mines ventouses réelles d'entraînement sur un disque d'un diamètre de 1 m suspendu dans le réservoir acoustique d'étalonnage de RDDC Atlantique à l'aide d'une perche rotative. Deux disques ont été examinés : un en aluminium et l'autre, en fibre de verre. Les disques ont été tournés au-dessous d'un projecteur à tube multimode fixe (MMPP) et d'un hydrophone. La géométrie a été configurée de sorte que les formes des mines paraissent directement sous le projecteur/l'hydrophone durant la rotation. Des mesures ont été prises à deux décalages du projecteur à disques et pour un arrangement légèrement bistatique. Différentes impulsions incidentes correspondant à différentes bandes de fréquences ont été étudiées. On montre que les formes des mines sont souvent faciles à distinguer de la réponse ambiante des disques en termes du temps de parcours et des caractéristiques (temporelles et spectrales) des échos.

14. KEYWORDS, DESCRIPTORS or IDENTIFIERS (Technically meaningful terms or short phrases that characterize a document and could be helpful in cataloguing the document. They should be selected so that no security classification is required. Identifiers, such as equipment model designation, trade name, military project code name, geographic location may also be included. If possible keywords should be selected from a published thesaurus, e.g. Thesaurus of Engineering and Scientific Terms (TEST) and that thesaurus identified. If it is not possible to select indexing terms which are Unclassified, the classification of each should be indicated as with the title.)

MMPP, mine, detection, broadband

This page intentionally left blank.

Defence R&D Canada

Canada's leader in defence
and National Security
Science and Technology

R & D pour la défense Canada

Chef de file au Canada en matière
de science et de technologie pour
la défense et la sécurité nationale

www.drdc-rddc.gc.ca